Overview of key results achieved in H2020 HighLite project helping to raise the EU PV industries' competitiveness

Tous, Loic; Govaert, Jonathan; Harrison, Samuel; Carrière, Carolyn; Barth, Vincent; Giglia, Valentin; Buchholz, Florian; Chen, Ning; Gordon, Ivan; More Authors

DOI
10.1002/pip.3667

Publication date
2023

Document Version
Final published version

Published in
Progress in Photovoltaics: research and applications

Citation (APA)
Tous, L., Govaert, J., Harrison, S., Carrière, C., Barth, V., Giglia, V., Buchholz, F., Chen, N., Gordon, I., & More Authors (2023). Overview of key results achieved in H2020 HighLite project helping to raise the EU PV industries' competitiveness. *Progress in Photovoltaics: research and applications*, *31*(12), 1409-1427. https://doi.org/10.1002/pip.3667

Received: 1 August 2022 | Revised: 30 November 2022 | Accepted: 19 December 2022

DOI: 10.1002/pip.3667

SPECIAL ISSUE ARTICLE

PROGRESS IN PHOTOVOLTAICS WILEY

Overview of key results achieved in H2020 HighLite project helping to raise the EU PV industries' competitiveness

Loic Tous[1,2,3] | Jonathan Govaert[1,2,3] | Samuel Harrison[4] | Carolyn Carrière[4] | Vincent Barth[4] | Valentin Giglia[4] | Florian Buchholz[5] | Ning Chen[5] | Andreas Halm[5] | Antonin Faes[6] | Gizem Nogay[6] | Hugo Quest[7] | Torsten Roessler[8] | Tobias Fellmeth[8] | Dirk Reinwand[8] | Hannah Stolzenburg[8] | Florian Schindler[8] | Max Mittag[8] | Arnaud Morlier[9] | Matevz Bokalic[10] | Kristijan Brecl[10] | Miha Kikelj[10] | Marko Topic[10] | Josco Kester[11] | Stefan Wendlandt[12] | Marco Galiazzo[13] | Alessandro Voltan[13] | Giuseppe Galbiati[14] | Marc Estruga Ortiga[14] | Frank Torregrosa[15] | Michael Grimm[16] | Julius Denafas[17] | Tadas Radavicius[17] | Povilas Lukinskas[18] | Tuukka Savisalo[19] | Thomas Regrettier[20] | Ivan Gordon[1,2,3,21]

Correspondence
Ivan Gordon, TU Delft, Mekelweg 5, 2628, CD Delft, Netherlands.
Email: ivan.gordon@imec.be

Funding information
European Union's Horizon 2020 Programme, Grant/Award Number: 857793

Abstract

The EU crystalline silicon (c-Si) PV manufacturing industry has faced strong foreign competition in the last decade. To strive in this competitive environment and differentiate itself from the competition, the EU c-Si PV manufacturing industry needs to (1) focus on highly performing c-Si PV technologies, (2) include sustainability by design, and (3) develop differentiated PV module designs for a broad range of PV applications to tap into rapidly growing existing and new markets. This is precisely the aim of the 3.5 years long H2020 funded HighLite project, which started in October 2019 under the work program LC-SC3-RES-15-2019: Increase the competitiveness of the EU PV manufacturing industry. To achieve this goal, the HighLite project focuses on bringing two advanced PV module designs and the related manufacturing solutions to higher technology readiness levels (TRL). The first module design aims to combine the benefits of n-type silicon heterojunction (SHJ) cells (high efficiency and bifaciality potential, improved sustainability, rapidly growing supply chain in the EU) with the ones of shingle assembly (higher packing density, improved modularity, and excellent aesthetics). The second module design is based on the assembly of low-cost industrial interdigitated back-contact (IBC) cells cut in half or smaller, which is interesting to improve module efficiencies and increase modularity (key for application in buildings, vehicles, etc.). This contribution provides an overview of the key results achieved so far by the HighLite project partners and discusses their relevance to help raise the EU PV industries' competitiveness. We report on promising high-efficiency industrial cell results (24.1% SHJ cell with a shingle layout

For affiliations refer to page 17

and 23.9% IBC cell with passivated contacts), novel approaches for high-throughput laser cutting and edge re-passivation, module designs for BAPV, BIPV, and VIPV applications passing extended testing, and first 1-year outdoor monitoring results compared with benchmark products.

KEYWORDS
BAPV, BIPV, H2020, IBC, photovoltaics, SHJ, silicon, VIPV

1 | INTRODUCTION

The European (EU) photovoltaic (PV) manufacturing industry has faced strong foreign competition in the last two decades while it also had to navigate through several boom and bust cycles. The first Renewable Energy Sources Act (or EEG in German) enacted by Germany in April 2000 kickstarted the whole EU PV industry by providing a set of feed-in tariffs (FITs) for 20 years and by introducing the 100,000 roofs program. The introduction of similar incentives in other EU countries in the mid-2000s quickly led to a boom in annual EU PV installations with numbers climbing from under 1 GW in 2000 to over 20 GW in 2011.[1] On the manufacturing front, several EU companies strongly benefited from this positive environment with Q-cells, a German company created in 2001, even taking in 2008 the top spot in the list of worldwide PV module manufacturers. However, global overcapacities in the PV industry driven by massive capacity additions in China led to very rapidly declining prices in the early 2010s across the whole PV value chain (polysilicon, wafer, cell, module, etc.). In addition, abrupt political decisions in several EU countries (Germany, Spain, Italy, etc.) to scale back or even suspend FITs eroded investors' confidence in PV. As a result, annual EU PV installations fell under 7 GW in 2016. The decision in 2013 by the EU to impose a minimum import price (MIP) on imports of PV modules from China did not resolve those issues with multiple EU PV manufacturing companies exiting the solar PV business or filing for bankruptcy. Despite all this, the EU PV community maintained its leadership in innovation in the 2000s and 2010s with several important developments such as diamond-wire sawing of monocrystalline silicon wafers,[2] various high-efficiency industrial solar cell concepts,[3–8] and advanced module designs[9–13] coming out of EU companies and/or research organizations.

Today the EU PV manufacturing industry is at an important crossroads given the recent global developments. On the one hand, after years of heavy competition from China, there is little manufacturing capacity left in Europe with less than 2 GW for ingots and wafers, around 1 GW for cells, and a bit more than 8 GW for modules.[1] On the other hand, continuous progress in the PV industry to improve efficiencies and decrease manufacturing costs[14] combined with the EU commission's decision to end the minimum import price (MIP) measures in 2018 have led to a boost in demand in the last few years. EU PV installations are now predicted to accelerate well above 30 GW per annum in the coming years given the high electricity prices and the need for Europe to quickly reduce its dependency from Russian oil and gas.[15] Finally, thanks to major progress in factory automation helping to reduce manufacturing costs[16] and with imported products being handicapped by high shipping costs (now representing over 10% of PV module costs), there is a lot more room today for EU companies to be competitive and generate sufficient profits to attract capital and grow.

To thrive in this competitive environment, the EU PV manufacturing industry needs to focus on highly performing PV technologies and products tailored for different applications. Distributed applications such as building-applied PV (BAPV), building-integrated PV (BIPV), and vehicle-integrated PV (VIPV) are particularly fast-growing markets due to the transition toward self-consumption and electro-mobility.[17] The EU PV manufacturing industry also needs to focus on reducing the environmental impact of its products (lower CO_2 footprint, improved sustainability, and recyclability, etc.) to differentiate itself from the competition and benefit from specific incentives that are already in place (e.g., CRE tenders in France) or that are being envisaged on a wider scale by the EU commission.[18] Finally, to avoid any major dependency on foreign products (as currently shown by the major crisis around Russian oil and gas supply) and to ensure local and responsible production following environmental, social, and governance (ESG) criteria, the EU PV industry must consolidate across its entire value chain (materials, equipment, etc.). In this context, existing EU PV manufacturers are ramping up production toward multi-GW scale while several new entrants are coming with very large plans (REC, Greenland, Carbon, etc.).

To further improve the competitiveness of the EU PV industry, leading EU PV institutes/universities have joined forces with major material, equipment, cell, and module manufacturers under the H2020 funded project called HighLite (GA no. 857793), which started in October 2019 for a duration of 42 months. The ambition of the HighLite project is to develop PV modules with high-performance, low-cost, and excellent environmental profiles that are tailored for various applications (BAPV, BIPV, and VIPV). This paper gives an overview of the key results achieved so far by the HighLite project partners and discusses their relevance to help raise the EU PV industries' competitiveness.

2 | APPROACH IN H2020 FUNDED HighLite PROJECT

The main idea of the HighLite project is to combine mature technologies developed by the project partners into innovative manufacturing solutions and products. The HighLite project focuses on bringing two

n-type c-Si technologies to high technology readiness levels (TRL 6–7) taking profit of the unique strengths and expertise of the project partners. The first one is based on shingle assembly of n-type silicon (Si) heterojunction (SHJ) cells. The second one is based on the assembly of industrial n-type Si interdigitated back-contact (IBC) cells cut in half or smaller. Shingle SHJ assembly using electrically conductive adhesives (ECA) enables the manufacturing of high efficiency PV modules that are lead (Pb) free, thereby meeting the European Union's Restriction of Hazardous Substances Directive (RoHS), and with superior temperature coefficients, aesthetics, and tolerance to partial shading.[12] On the other hand, modules with high-efficiency IBC cut-cells are particularly interesting for applications such as BIPV and VIPV, which are particularly demanding in terms of modularity and aesthetics. Both SHJ and IBC cells can be produced from thinner Si wafers (100–160 µm compared with 140–200 µm for standard p-type Si cells) without compromising cell efficiencies and yields as shown by the project partners in previous funded projects.[5,16] This allows to produce SHJ and IBC modules with much lower CO_2 footprints particularly if one selects poly-Si/wafer suppliers from the low-carbon footprint EU supply chain.[19]

As shown in Figure 1, the overall objectives of HighLite, which were set in late 2018, are to (i) develop innovative solutions and processes up to TRL4–5, (ii) develop innovative PV equipment and materials for the assembly of thin (100–160 µm after texturing) cut-cells, and (iii) demonstrate high-efficiency solar cells and modules in pilot production.

2.1 | High efficiency n-type SHJ and IBC cell concepts

A first major objective is to develop SHJ cells with a shingle metallization layout with efficiencies ≥23.5% on full M2-size wafers and ≥23.3% on ¼ (or smaller) cut-cells. On the one hand, the SHJ cell efficiency objective on full-size is no longer very impressive given the rapid rate of progress in the industry as the latest world record SHJ cell is now reaching an externally confirmed efficiency of 26.5%.[20] On the other hand, it is important to remember that (i) grid resistive losses are neglected in most external calibration results and (ii) a shingle metallization layout induces significant resistive losses at cell level due to the deported busbars design (see Figure 2A). In addition, this objective is for cells produced at CEA-INES SHJ pilot-line, which uses relatively older processing equipment and automation solutions together with n-type Si wafers in M2 format (156.75 mm). Therefore, improvements obtained in the project are expected to be transferable to the latest generation SHJ production lines which are making use of advanced equipment and higher quality n-type Si wafers in M10 (182 mm) or G12 (210 mm) formats. More importantly, reaching efficiencies that are only 0.2%$_{abs.}$ lower after cutting the SHJ cells into small segments would represent a major achievement since cutting losses are one of the main factors limiting the efficiency of SHJ shingled modules.[21,22]

A second major objective of this project is to fabricate low-cost IBC solar cells with efficiencies of 24.5% on full-size (6-in.) and 24.3% on ¼ size or smaller using advanced ZEBRA (the IBC concept developed by the research institute ISC Konstanz) and POLO-IBC (poly-Si on oxide IBC) cell concepts with passivated contacts. Key features of standard ZEBRA cells without passivated contacts include (i) gap-less design for process simplification and uniform breakdown, (ii) simple BBr_3 and $POCl_3$ diffusions with SiO_2/SiN_x passivation, and (iii) screen-printing of a multilayer silver (Ag) metal grid (as shown in Figure 2B) to simplify cell interconnection at module level.[22] The approach in HighLite is to develop an advanced ZEBRA cell design with passivated contacts in order to significantly reduce recombination losses.[23,24] Key features of POLO-IBC cells include (i) the use of lower cost

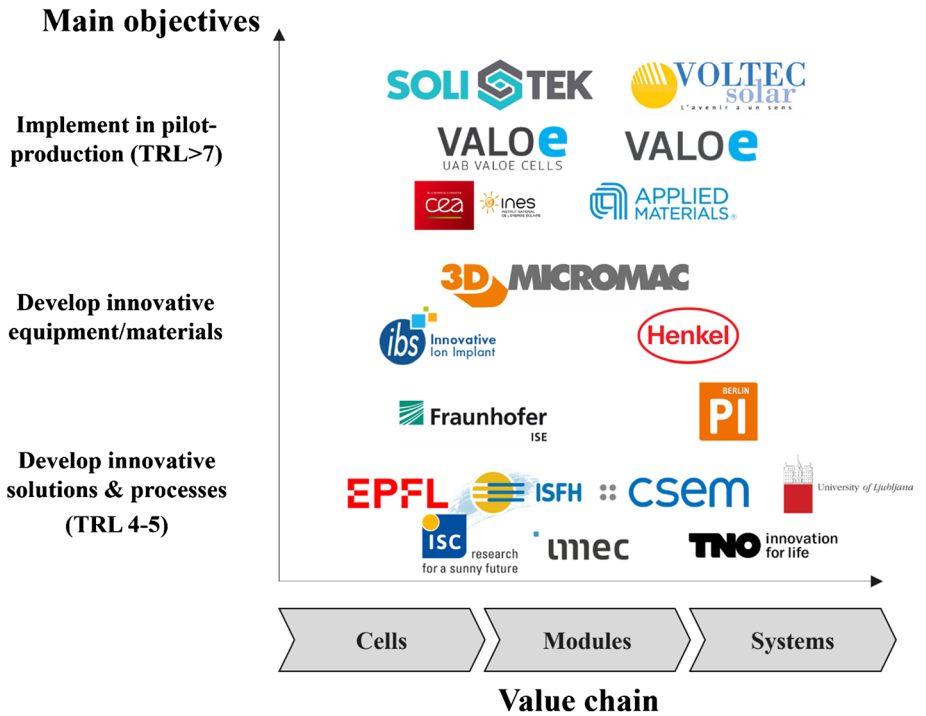

FIGURE 1 Main objectives of HighLite project partners along the value chain [Colour figure can be viewed at wileyonlinelibrary.com]

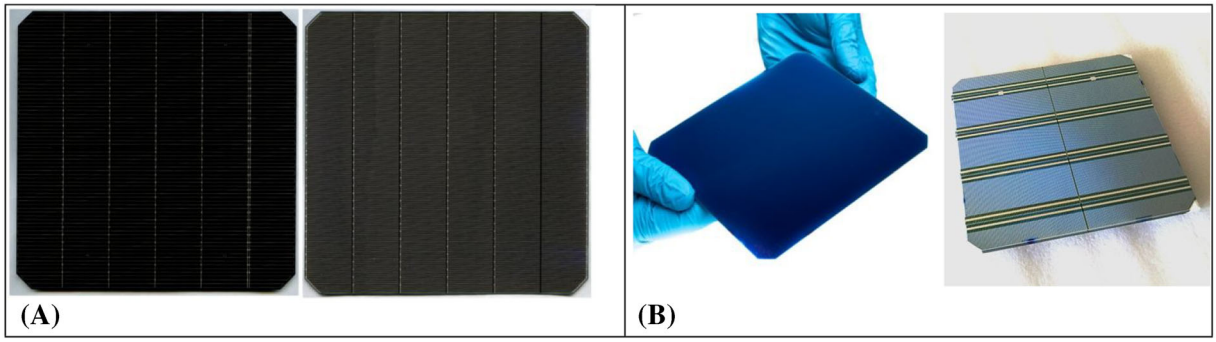

FIGURE 2 (A) M2-size SHJ cell with a six-segment shingle metallization layout at the front (left image) and rear (right image) sides and (B) M2-size ZEBRA IBC solar cell with no metallization at the front (left image) and a 2× 4 busbars (2×4BB) half-cut layout at the rear (right image). [Colour figure can be viewed at wileyonlinelibrary.com]

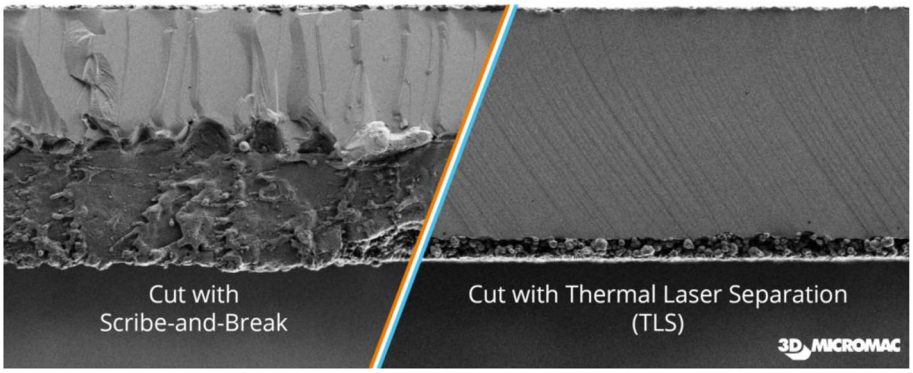

FIGURE 3 Scanning electron microscopy (SEM) images of silicon solar cells after typical cutting using laser scribing from the bottom side and mechanical breaking (left) and after using 3D-Micromac proprietary thermal laser separation (TLS) approach (right). TLS results in smooth cutting through both the silicon wafer and bottom Al metallization paste unlike the scribe-and-break approach. [Colour figure can be viewed at wileyonlinelibrary.com]

p-type wafers, (ii) n-type doped passivating contacts using POLO technology, and (iii) the absence of BBr_3 diffusion since the local p^+ emitter is formed by screen-printing of aluminum (Al) paste and subsequent alloying with the Si bulk during fast firing.[25] The approach in HighLite is to further develop the POLO-IBC concept and upscale it to large format wafers. In both cases, the implementation of passivated contacts using simple and cost effective methods is crucial to maximize cell efficiencies without compromising costs and yield losses. Therefore, the HighLite project partners first focused on identifying the most industrially feasible approaches for producing high-temperature passivating contacts compatible with standard screen-printing metallization (firing-through) before looking at ways to implement them in the advanced ZEBRA and POLO-IBC concepts.

2.2 | Advanced laser cutting and edge re-passivation approaches

Cutting cells in two ("half-cut"), three ("tri-cut"), or even more segments for shingling technology (typically five to seven segments depending on the cell concept and format) is attractive to improve packing density and reduce interconnection losses at module level but presents multiple challenges. First, it causes significant efficiency losses at cell level.[21,22] Second, it can lead to cell breakage during module processing (interconnection, lamination, etc.) causing significant yield losses or during module shipping and installation with micro-cracks rapidly propagating in the field due to wind loading and thermal cycling.[26] Finally, it can also accelerate longer term degradation issues in the field (hot spots, snail trails, etc.).

In HighLite, three different cell cutting approaches are being optimized by the project partners through experiments as well as advanced characterization and modeling. The first approach is based on optimizing traditional laser scribing and mechanical breaking for SHJ shingled and IBC cut cells since it is the most adopted method in the industry today. Typically, this method requires a deep scribing of approx. 30%–50% of the wafer's thickness and causes significant damaging of the solar cell edges in combination with microcracks. The second approach is based on 3D-Micromac proprietary thermal laser separation (TLS) technology. TLS relies on initiating a small crack at the wafer edge using a laser and then propagating it through the entire cell using a well-defined and controlled stress field imposed by a laser-based heating and subsequent water spray cooling system. This approach is already well established in the PV industry for cutting cells in half.[27] Major benefits include the creation of a smooth wafer edge (see Figure 3) and the possibility to cut cells inline without any mechanical contact. A major challenge that is addressed in HighLite is to achieve five to seven cuts per cell (needed for shingling) without compromising throughputs or yields. The third alternative and innovative approach is based on 45° rotated ingots as proposed by CEA-INES. The main idea is to square the initial wafer ingot with a 45°

rotation compared with the standard practice in the industry so that crack propagation along (110) planes can occur naturally parallel to the metal lines instead of diagonally. The main benefits are the creation of very smooth wafer edges (similar to TLS) using a simple crack initiation at the edges and the possibility to achieve very high throughputs. The main challenge is to avoid spontaneous crack initiation during cell or module processing.

2.3 | Automated assembly of cut-cells

Various solutions are being explored by the project partners for the assembly of SHJ shingled and IBC cut-cells. Shingle assembly, which was first patented by Dickson in 1960, has regained a lot of momentum recently thanks to developments made by companies such as Solaria and Sunpower among others.[13,28] The main idea with shingling assembly is to eliminate visible interconnects and increase packing density (putting more cells per module) by using an adapted cell metallization layout (see Figure 2) so that cut cells can be overlapped slightly (similar to roof shingles) and series connected using ECAs. While there are several manufacturers commercializing shingled modules based on lower efficiency p-type cells, there are still several issues that need to be resolved when using higher efficiency SHJ cells. First, shingling technology requires very conductive fingers which are more difficult to obtain in SHJ cells using low temperature Ag metallization than in conventional p-type devices. Second, ECA formulation and consumption needs to be further optimized to reduce costs without compromising long-term reliability. Third, throughput and yield losses need to be improved to compete with other interconnection techniques such as tabbing-stringing of copper (Cu) ribbons or wires. As for the assembly of IBC cut-cells, the main ambition of the HighLite project partners is to further develop approaches based on tabbing-stringing of flat Cu ribbons (or round Cu wires) or conductive backsheet (CBS) technology.[13,28] The main benefits of using CBS technology in combination with IBC cut-cells include: (i) excellent aesthetics, (ii) lower cell-to-module losses, and (iii) improved temperature dissipation compared with other approaches. The main difficulty is to master accurate placement of small IBC cut-cells (needed to improve modularity) while achieving sufficiently high throughputs and yields.

2.4 | Tailored PV module designs

Another major ambition of this project is to develop new PV module designs that are specifically tailored for BAPV, BIPV, or VIPV applications. For BAPV, apart from reaching specific cost targets, one of the final objectives of the project is to demonstrate PV modules with excellent aesthetics, high efficiency ($\eta \geq 22\%$), and very low carbon footprint (≤250 kg-eq.CO_2/kWp). For comparison, most modules for BAPV applications are currently based on p-type passivated emitter and rear cell (PERC) technology with module efficiencies in the range of 19.5–21.5% and carbon footprints in the range of 500–1200 kg-eq.CO_2/kWp depending on the calculation method.[19] For BIPV, the objective is to demonstrate module efficiencies $\eta \geq 21\%$ while achieving superior optical appearance and improved tolerance to partial shading. Finally, the objective for VIPV applications is to demonstrate 3D-curved vehicle-integrated PV modules with $\eta \geq 20\%$ and a weight ≤ 5 kg/m^2, which are both crucial to enable VIPV integration in passenger car body parts (bonnets, doors, etc.) and in other vehicle types (commercial vans, heavy trucks, and trailers, etc.). For each of these applications, the HighLite project partners have been looking at ways to reduce manufacturing costs, pass critical reliability tests (such as thermal cycling [TC], damp heat [DH], vibration, etc.), and improve operation under non-ideal conditions (elevated temperatures, high amounts of diffuse light, partial shading, etc.). For this, multiple demonstrator modules have been produced by the HighLite project partners and benchmarked against commercially available modules using both indoor and outdoor testing.

In the following section, we discuss the key results obtained by the HighLite project partners after 32 months of joint developments.

3 | RESULTS AND DISCUSSIONS

3.1 | High efficiency n-type SHJ cells at pilot line level

More than 10,000 high-efficiency M2-size SHJ cells have been produced so far at CEA-INES pilot-line to support developments planned by the HighLite project partners. In the course of 2021, CEA was able to significantly ramp-up the cell efficiencies obtained, especially by reducing defectivity[29] and optimizing the Ag metallization on both sides without compromising cell-to-module losses or reliability.[30] First production batches showed efficiencies in the 22.6–22.8% range with the latest batches using an adapted production flow resulting in average efficiencies over 23.3% and an externally confirmed best cell efficiency of 24.1% (see Figure 4) exceeding one of the key efficiency targets. Additional batches were also produced to demonstrate together with applied materials (AMAT) the feasibility of adapting the metallization layout and subsequent automated shingle assembly to reduce the shingle overlap from the 1–1.5 mm typically used in the industry down to 0.5 mm with significant benefits in terms of potential cost reduction and efficiency improvements at module level.[31] More recently, CEA could show the feasibility of making high efficiency SHJ shingle cells at pilot level using low carbon EU-made wafers with a starting thickness of 90–100 µm (instead of 120–160 µm) while achieving sufficiently high yields during cell manufacturing and shingle assembly. This works paves the way to BAPV modules with >22% efficiencies and a carbon footprint 250 kg-eq.CO_2/kWp. Finally, to address growing concerns associated with Ag metallization costs and availability of Ag at Terawatt level,[32] CEA has also been recently showing promising results to drastically reduce the amount of Ag used at both cell level (by replacing Ag with copper) and at module level (by reducing the consumption of Ag-based ECA).[31,33]

As shown in this subsection, very high cell performances can be achieved for SHJ shingles despite the additional metallization

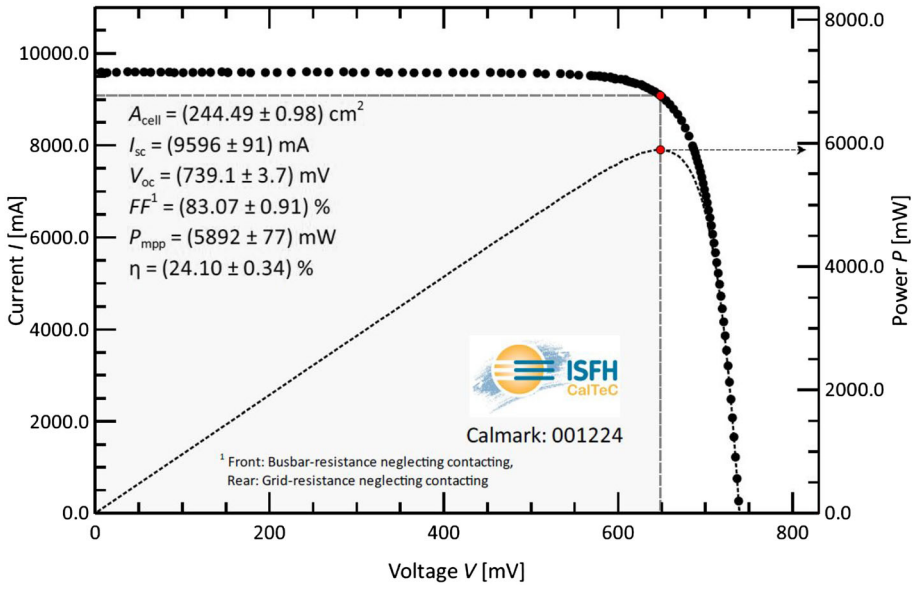

FIGURE 4 Externally confirmed efficiency of 24.1% for a full area M2-size (area = 244.5 cm²) SHJ cell with a shingle metallization layout produced at CEA-INES pilot-line in 2021 [Colour figure can be viewed at wileyonlinelibrary.com]

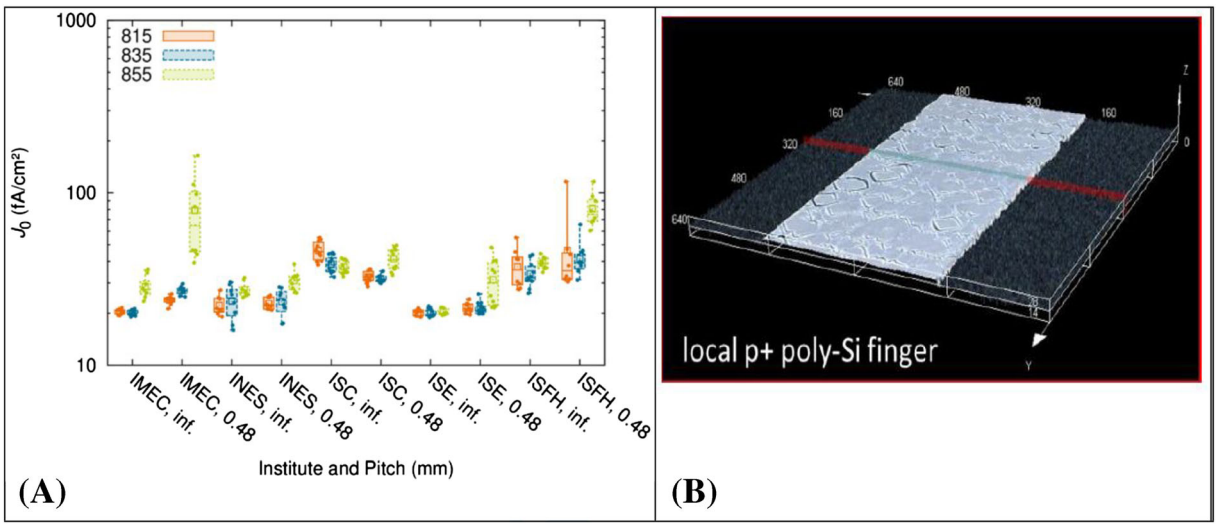

FIGURE 5 (A) Total dark saturation density J0 for TOPCon samples with (0.48 mm finger pitch) and without metallization (infinite finger pitch) for different set peak firing temperatures in the range of 815–855°C.[34] (B) Laser scanning microscope image of local p^+ poly-Si finger surrounded by textured silicon surface produced by a novel laser crystallization step for maskless structuring of p^+ poly-Si.[24] [Colour figure can be viewed at wileyonlinelibrary.com]

constraints linked to the deported busbar design. Current design and process are believed to already be perfectly suited for major coming industrial PV evolutions such as larger size and/or thinner wafer use on production lines. However, further work is still needed to prove at both cell and module level, that the alternative metallization schemes currently under development and mandatory for cost competitiveness and long-term sustainability of the technology are also fully compatible with the specific constraints linked to shingle interconnection.

3.2 | Development of advanced IBC cells with passivated contacts

As with SHJ cells, more than 10,000 low-cost IBC cells in M2 and G1 formats have been produced by Valoe Cells for the project using standard ZEBRA technology licensed from ISC Konstanz. Latest batches using high-quality n-type wafers in G1 format are now giving average cell efficiencies above 23.0% with results mainly limited by recombination losses as also reported by other companies using ZEBRA technology.[23]

Various approaches have been investigated by the HighLite project partners to implement passivated contacts and reduce recombination losses in IBC cells. In a first step, a large round-robin experiment involving five of the leading EU PV institutes was organized by Fraunhofer ISE to evaluate various tunnel oxide passivated contacts (TOPCon) layers prepared by plasma enhanced chemical vapor deposition (PECVD) or by low pressure chemical vapor deposition (LPCVD) and using various dielectric capping layers. For all the approaches, dark saturation current-densities ranging between 2 and 10 fA/cm² as shown in Figure 5A and contact resistivities below 10 mΩ.cm² have

been achieved.[34] Additional characterization based on scanning spreading resistance microscopy (SSRM) revealed that many of those optimized layers feature local regions of doping enhancement favoring current transport.[35] The fact that similar results can be realized by multiple institutes using different approaches and equipment is expected to drive costs down and contribute to the increased adoption of TOPCon technology in various cell concepts.[36] In a second step, the HighLite project partners focused on the implementation of polysilicon (poly-Si) based passivated contacts in low-cost IBC solar cells. A key challenge is to develop suitable and industrially feasible processes which do not infringe with the multiple patents already owned by companies such as Sunpower among others. This is why several novel approaches have been investigated by the project partners including: (i) POLO-IBC technology,[25,37] (ii) local patterning using plasma immersion implantation,[38] (iii) PECVD deposition of doped layers via shadow masks,[39] and (iv) laser structuring for advanced ZEBRA cells[24] as shown in Figure 5B. So far, the most promising results obtained include cell efficiencies up to 23.92% (externally confirmed) with open circuit voltages around 720 mV for POLO-IBC technology on small area p-type wafers and efficiencies up to 23.5% (internal measurement) for advanced ZEBRA n-type cells using polysilicon passivating contact layers on both polarities on full area M2 (area = 244.3 cm^2) format. In both cases, further developments are planned to reach the ≥24.5% cell efficiency target before the end of the HighLite project in March 2023.

3.3 | Advanced characterization of edge losses before and after edge re-passivation

The basis for cut edge induced performance loss evaluation was the round robin of full and half-cells cut by laser ablation and cleaving (L&C) and thermal laser separation (TLS) that was carried out by the partners at the beginning of the project. Results revealed small but not negligible losses in performance of cut half cells (0.5–1.5 mV in V_{oc} and 0.5–0.75%$_{abs}$ in pFF).

Aiming to better understand these losses, partners applied various advanced spatial characterization methods combined with electrical and optical simulations for characterization of cut edge induced recombination. UL used wavelength dependent laser beam induced current measurements (LBIC(λ), Figure 6A) and injection-dependent electroluminescence (EL(*J*))[41] to calibrate newly developed combined rigorous optical and electrical simulation model (developed in Sentaurus T-CAD and in-house CROWM simulator). The results show, that for laterally inhomogeneous solar cells, optics plays a more important role in shaping the results than electrics. Thus, the effects of optics must not be neglected, but properly evaluated, otherwise solely relying on electrical simulation may bring erroneous or misleading conclusions.[42–44] Fraunhofer ISE focused on injection dependent photoluminescence (PL(*I*)) measurements of precursors, host cells, and cut cells and simulated the circumstances in Quokka3. The approach distinguishes between cut bulk and cut junction recombination described by edge surface recombination velocity ($S_{eff,edge}$) and dark saturation current ($J_{02,edge}$), respectively.[45] This allows evaluation of different cutting techniques as well as a sensitivity study of performance parameters' decrease due to different cut edges. ISC also used PL(*I*) and Quokka3 simulations but focused on IBC cells and a variety of different cut cell sizes (1/1, 1/2, 1/4, 1/8) including 1 or 2 side cut and cut over n + or p + region. The smallest cut cell, with 2 side cut over the emitter (p+) region is the most affected by the cut.[46] It showed (experimentally proven) that the inherent feature of IBC cells to allow for sparing the emitter upon cutting vastly reduces the cut cell losses. Similar conclusion was drawn by CEA, where they used Silvaco Atlas package to simulate cut cell performance using their three-unit cell model that distinguishes between a core unit cell, a native edge cell, and a cut edge cell, where recombination of different surfaces of unit cells are described by a defective interface density.[21] Collectively, the partners prepared a comprehensive toolbox of characterization and simulation approaches to support developments in the cut edge repassivation task.

In parallel, various edge repassivation approaches have been evaluated in the course of the project. Most partners focused on using

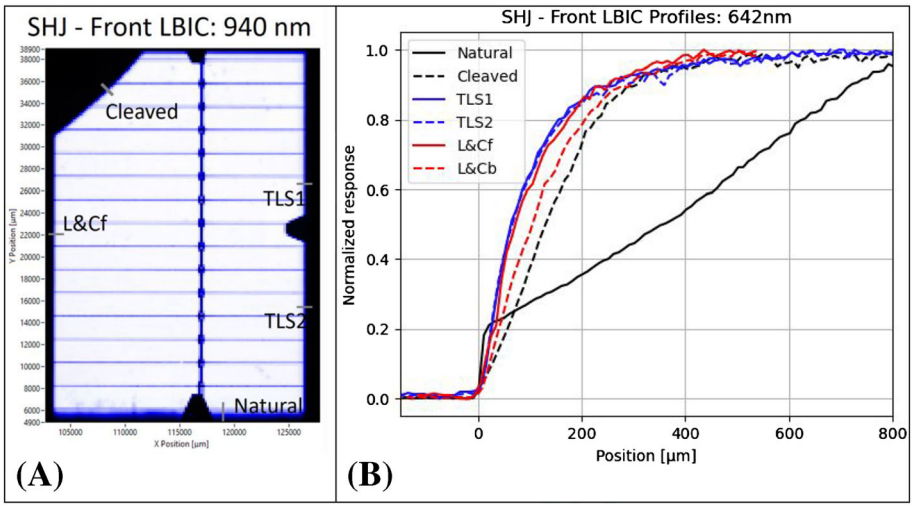

FIGURE 6 (A) LBIC image of SHJ cell cut using mechanically cleaving, laser scribe and cut (L&C), and thermal laser separation (TLS). *Source*: Bokalic et al.[40] (B) LBIC response across the cut edges for the different positions marked in (A). *Source*: Bokalic et al.[40] [Colour figure can be viewed at wileyonlinelibrary.com]

either aluminum oxide (AlO_x) deposited by Atomic Layer deposition (ALD), or silicon nitride (SiN_x) layers deposited by PECVD, introduced at the end of the process. Indeed, the idea is to combine potential light management improvement thanks to the double anti-reflective (ARC) layer coating generated, with improved passivation observed on the cut-edge generated. However, for SHJ cells, the temperature limitations are a major constraint, strongly limiting the passivation properties of the layers considered. Nevertheless, very promising results have been achieved by Fraunhofer ISE,[47] CEA,[33,48] and ISC[49,50] who demonstrated the feasibility of achieving high levels of re-passivation and maintaining this gain in performance after module fabrication. Of note, CEA recently achieved very high recovery levels for shingle SHJ cells (up to 90% of initial ŋ), which are among the best reported values on PV cut-cells, no matter the cell technology.[48] Other approaches that were optimized by the partners include the use of plasma immersion implantation of hydrogen and chemical passivation using novel passivating agents such as perfluoro(2-(2-sulfonylethoxy)propyl vinyl ether)-tetrafluoroethylene copolymer, also referred to as "Nafion."[49,50] This approach provides excellent passivation of the edges, can be carried out at room temperature without the need of vacuum, and results in stable repassivation that can be used in mass production. A major learning made by the HighLite project partners is that it is absolutely key to have smoothly cut edges (as made possible with TLS or with the 45° rotated ingot approach of CEA but not with L&C) and to minimize the time between cutting and re-passivation to achieve the best results. Overall, the results obtained by the HighLite project partners demonstrate the feasibility of using edge re-passivation to maximize performance at cell and module level, but further developments are still needed to industrialize those various approaches and implement them in production.

3.4 | Novel high-throughput TLS dicing and shingle assembly tools

Another major achievement has been the development by 3D-Micromac of a completely new production equipment providing a free choice of cell cutting layouts that range from half to shingled cells without compromising throughput or yield. The new tool, called microCELL™ MCS, is based on a novel circulating chuck system with 22 carriers enabling gross throughputs >6000 wph for 1/2 to 1/6 cut-cells. It is characterized by a compact footprint (as shown in Figure 7A) and a very high degree of freedom in terms of wafer format (M2 to M12) and cutting layouts thanks to the use of a flexible chuck design and the possibility to add up to five process stations (see Figure 7B). This tool retains all the major benefits of TLS technology including high yield, reduced generation of micro-cracks, and hot spots,[51] and smooth cut edges which are key for subsequent edge re-passivation. It can be inserted inline (with additional automation) or operated as standalone using high-throughput automatic loading/unloading equipment also developed by 3D-Micromac in HighLite (see Figure 7C). Given the multiple benefits compared with other competing solutions for high-throughput laser cutting, 3D-Micromac expects that the new microCELL™ MCS tool will become its next successful laser tool in the EU and global PV markets.

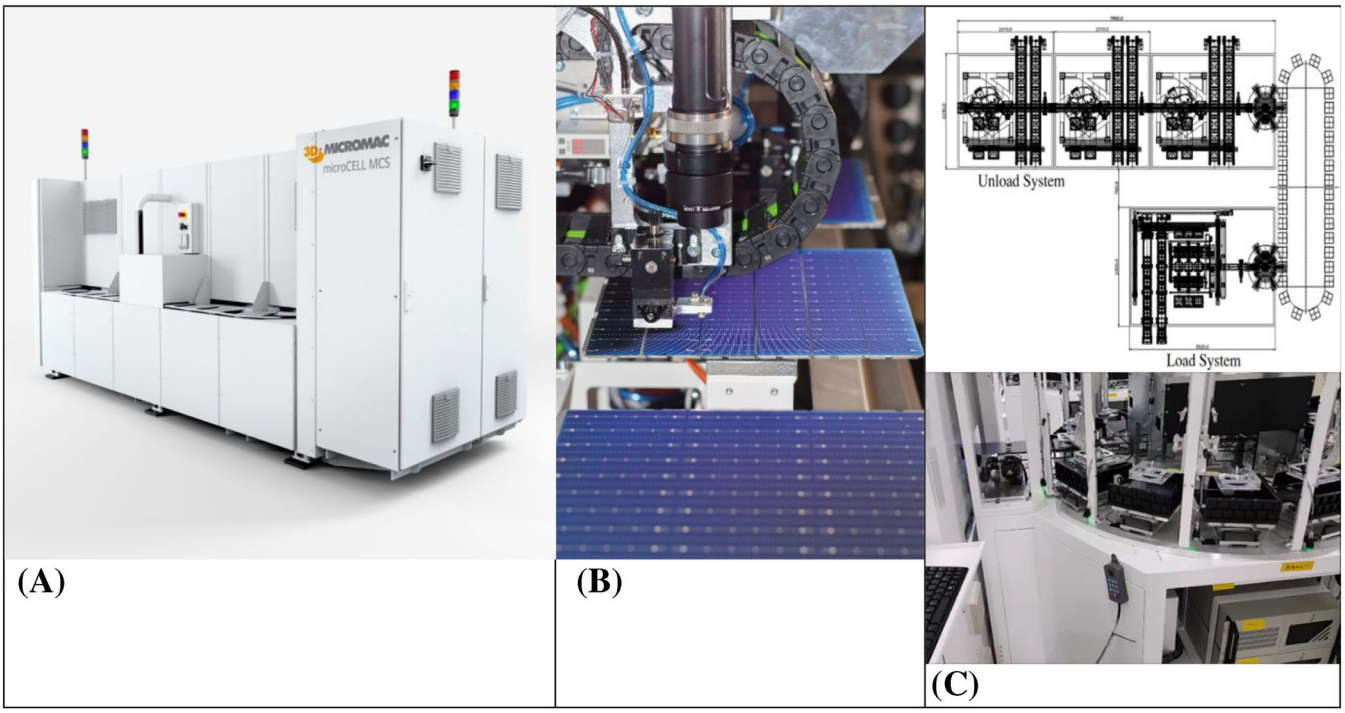

FIGURE 7 (A) microCELL™ MCS high-throughput shingling tool developed by 3D-Micromac in HighLite, (B) view of one of the process station, (C) top: schematic of automatic system for standalone operation of the microCELL™ MCS with high-throughput loading of full wafers and unloading of shingles into dedicated trays, bottom: partial view of the loading system [Colour figure can be viewed at wileyonlinelibrary.com]

In order to enable the process flow based on TLS technology, which is one requirement for edge repassivation of SHJ cells, AMAT's Sonetto™ shingle assembly equipment had to be significantly modified. In fact, input material to the assembly tool changes from full cells to cut shingles. AMAT and 3D-Micromac developed a common interface to transfer stacks of shingles from one tool to the other, with buffering and sorting to separate full size shingles from chamfered ones. Multiple shingles are loaded and aligned, ECA printed with a single stroke and then transferred to the assembly module where they are overlapped and cured in an inline oven. This equipment has the capability to reach a gross throughput of 6000 wph (M12 cell format) and features automated ECA based connection of string ribbons (see Figure 8A) as well as inspection metrology for alignment and print quality. To prove the robustness of the solutions implemented on this tool, AMAT tested aggressive configurations using special SHJ cells produced by CEA. Specifically, multiple batches of 90 µm thick cells and shingles in M2 format have been successfully processed and the handling system was optimized. An important metric for assembly precision is the minimum shingle overlap, and to prove it AMAT processed shingles with a layout suitable for 0.5 mm. By changing vision recipes and axes parametrizations, it was possible to realize these strings and prove the current gain related to the increased exposed area against the current best known method.[31] Overall, the strings made by AMAT were successfully used by the HighLite project partners to tailor PV modules for various applications including BAPV, BIPV, and VIPV as discussed in the next sections.

3.5 | Flexible and automated assembly of IBC cut-cells

Several approaches for flexible and automated assembly of IBC cut-cells have been developed in the course of the project mainly by partners Valoe and ISC with the support of other project partners. Valoe has been working on a novel assembly line called HAMA that is based on conductive backsheet (CBS) technology using offline ECA printing, inline cell cutting, and a high-speed delta robot that is capable to make more than 4000 picks per minute for the final assembly (see Figure 9A). Today, this new line is being successfully used to produce a wide range of unconventional odd form IBC modules for various applications such as BAPV, BIPV, and VIPV (see example in Figure 9B). In parallel, Valoe has also been developing a flexible and automated line to manufacture bifacial glass–glass IBC modules (Valoe's Crystal Twin) using a new concept to create a low cost transparent CBS. Promising first results have been obtained using 144 half-cut ZEBRA IBC cells in G1 format with cell-to-module ratios in the range of 98 to 100% for a bifacial glass–glass design (see Figure 9C). Finally, ISC has been working on multi-busbars (MBB) soldering of half-cut ZEBRA IBC cells in G1 format using adapted tabbing-stringing equipment from Teamtechnik. Again, promising results have been obtained with CTM ratios in the range of 99 to 101% using a monofacial glass/white backsheet design. Of note, ISC has been exploring the possibility to slightly overlap the IBC cut-cells during tabbing-stringing to form gapless strings and even overlap strings during module layup to form a fully gapless design. This has the potential to improve

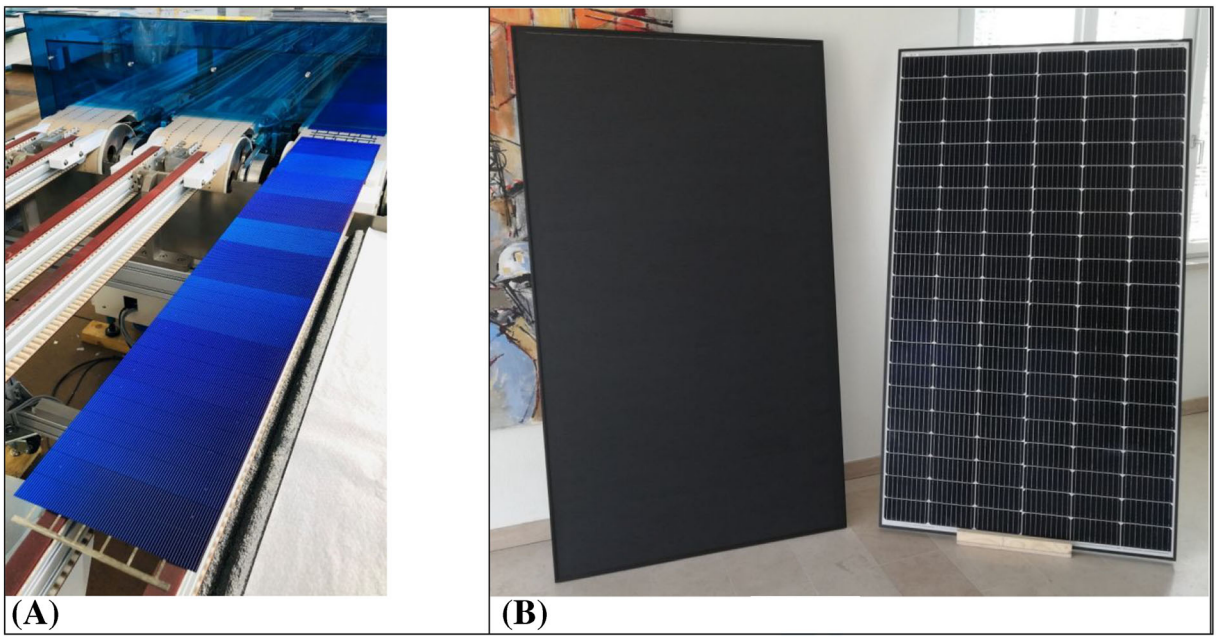

FIGURE 8 (A) Finished string of 39 full size SHJ shingles with the string ribbons also attached in the applied Sonetto™ tool. *Source*: AMAT. (B) Left: Shingle full black module with 4 mm thick glass for BIPV, right: reference Tarka 120 module with 9BB design. *Source*: Voltec Solar [Colour figure can be viewed at wileyonlinelibrary.com]

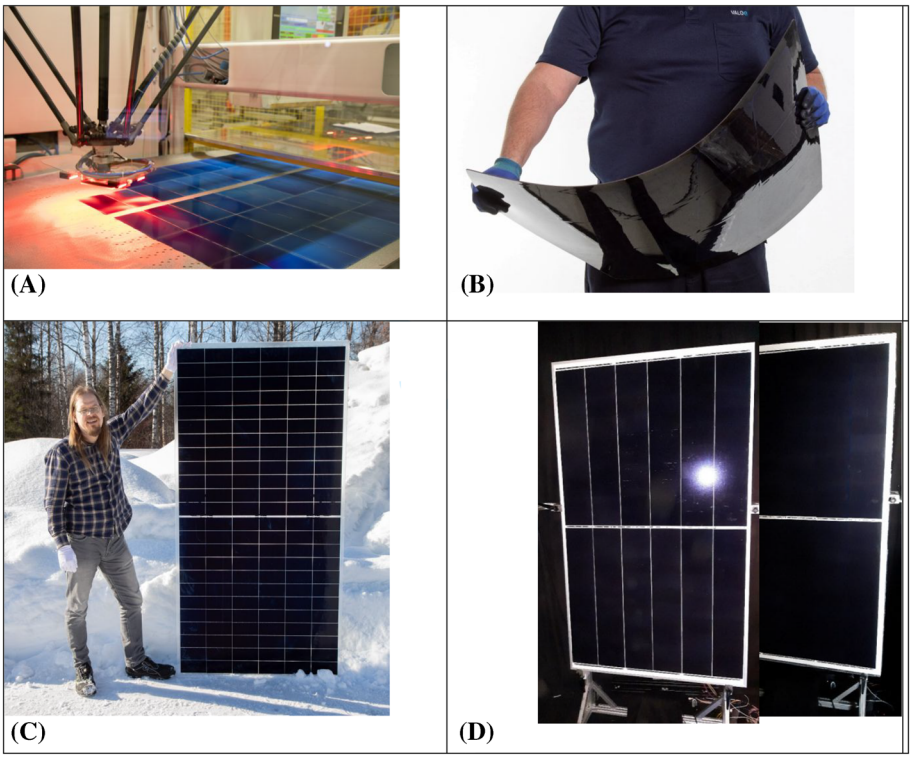

FIGURE 9 (A) High speed delta robot in HAMA line. *Source*: Valoe. (B) Flexible odd form IBC module for VIPV application. *Source*: Valoe. (C) Bifacial glass–glass Chrystal Twin module with 144 IBC half-cut. *Source*: Valoe. (D) Monofacial glass-backsheet modules from IBC using either gapless strings (left) or a fully gapless (right) design. *Source*: ISC[52] [Colour figure can be viewed at wileyonlinelibrary.com]

aesthetics even when using a white backsheet design (see Figure 9D) and enable full area module efficiencies above 22% when combined with smaller front glass dimensions.[52]

3.6 | Tailored PV module designs for BAPV

As briefly shown in the previous sections, the HighLite project partners have been developing advanced assembly equipment for SHJ and IBC cut-cells allowing to tailor PV modules for a wide range of applications. In this section, we discuss further the developments made by Fraunhofer ISE to improve cell-to-module (CTM) analysis of various BAPV designs and by CEA to improve the reliability and cost of SHJ shingled modules targeting BAPV.

BAPV modules currently show large similarities to modules for utility-scale PV power plants but are typically smaller (i.e., 60 full cell equivalents instead of 72) to keep the module weight under 20 kg and increase modularity which are both key in sloped residential roofs. Within HighLite, Fraunhofer ISE has been performing simulations using the CTM-methodology: a bottom-up, multi-physics loss channel analysis based on the modeling of module components and their interaction in PV modules. Simulations are performed based on material data (e.g., spectrally resolved reflectance, specific resistance, etc.) and specific module designs (e.g., geometrical data such as solar cell spacing). Overall, the analysis revealed that the optimal number of busbars on cell level is rarely identical with the optimal number of busbars considering module effects thus providing motivation for a holistic thinking.

One of the key results achieved by Fraunhofer ISE is the extension of models to cover various types of interconnections such as (i) edge connectors, (ii) flat ribbons, (iii) round wires, and (iv) CBS technology.[53] Another key result is the detailed CTM analysis of various commercial benchmark products (Voltec Tarka 120, etc.) and many different SHJ shingle and IBC cut-cells module configurations which greatly helped accelerate the developments by the project partners working on BAPV but also BIPV and VIPV products. One such example is given in Figure 10 where CTM analysis was performed for a 60-M2 cell equivalent SHJ shingled module for BAPV application. In the non-optimized case, the starting cell efficiency was 22.77% (after cutting), the cell overlap 1 mm, and the string gap 3 mm. CTM losses in terms of efficiency are typically small and mainly caused by the necessary module edge area that is needed for interconnection and to pass critical reliability tests such as Damp Heat testing. Nevertheless, improving the full area module efficiency from 21.21% to 22.45% appears feasible with the following improvements: (i) higher starting cell efficiency of 23.29% (assuming successful edge re-passivation), (ii) reducing the cell overlap to 0.5 mm and the string spacing to 1 mm (both allowing to reduce the full module area), and (iii) improving the reflectivity of the rear side cover in the infrared.

After specific developments of shingling technology conducted in the first months of the project, CEA has proven that promising first outcomes could be fully compatible with industrial constraints. For this full size modules were assembled with 12 vertical strings (2×6 parallel strings in series, all produced using the Applied Sonetto™ tool), integrating 39 SHJ shingles tiles, corresponding to 78 M2-size cells per module. One module was manufactured in 2021 using a glass/

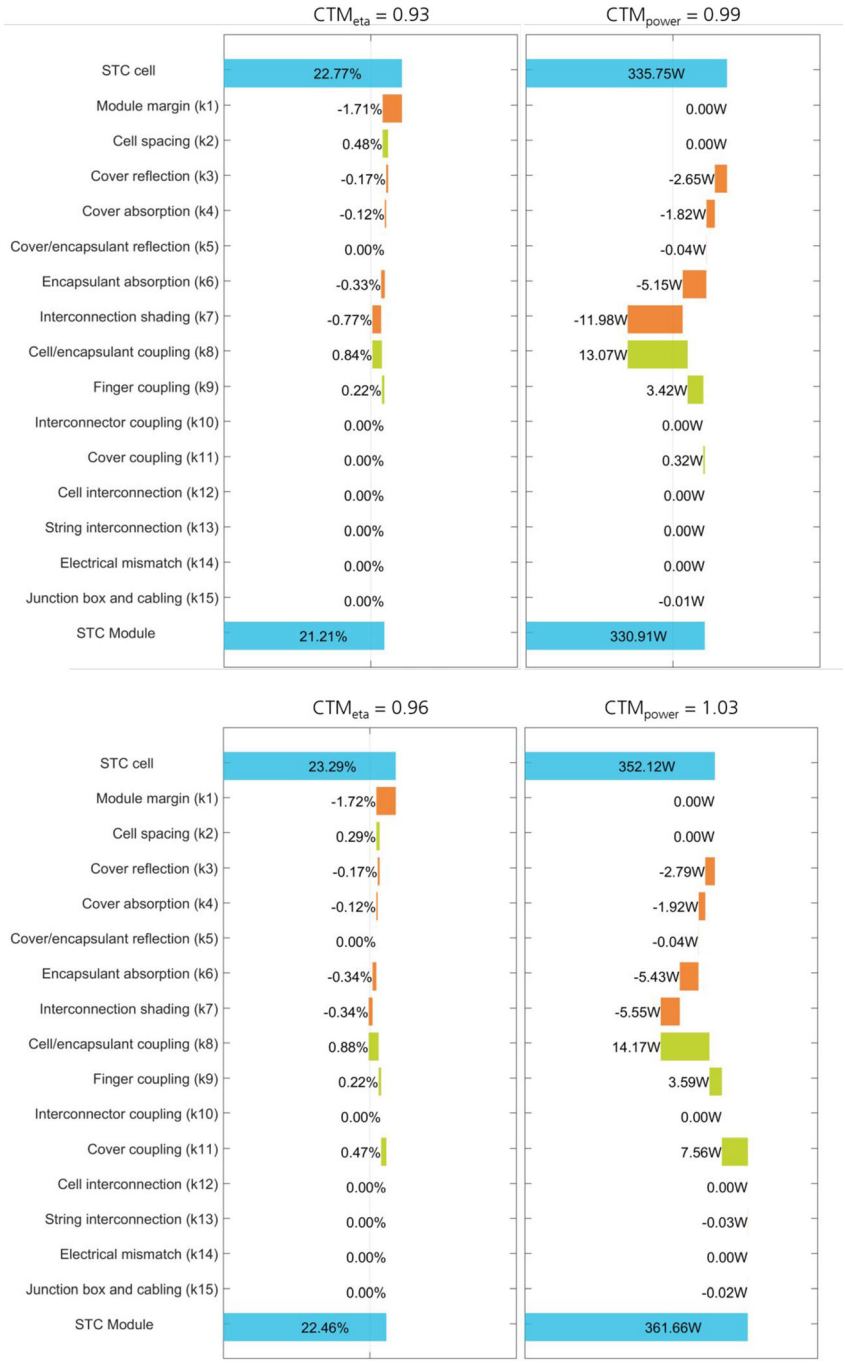

FIGURE 10 (Top): CTM-analysis of efficiency and power for 60-cell equivalent BAPV SHJ shingle module with non-optimized cell and module design. (Bottom): Similar CTM-Analysis for an optimized BAPV SHJ shingle design. *Source*: Fraunhofer ISE [Colour figure can be viewed at wileyonlinelibrary.com]

transparent backsheet design leading to a power output (P_{max}) of 400 W_p and a full area module efficiency of 20% (area = 1.99 m^2) together with 85% bifaciality. Another 78 M2-cell equivalent module with a black backsheet was produced to show the benefits in terms of aesthetics with a P_{max} still around 390 Wp. Finally, multiple 60 M2-cell equivalent modules with a glass–glass design were produced by CEA (see Figure 11A) giving an average P_{max} of 322 Wp and an active area efficiency of 21.5%. Outdoor testing results using those modules compared with benchmark commercial products are detailed in Section 3.9.

In parallel, CEA optimized the overall interconnection assembly with regards to the IEC requirements, with a specific focus on Thermal Cycling (TC) tests (−40°C/85°C). Again, outstanding reliability outputs were achieved with about only 1% loss in P_{max} measured on all modules produced for up to 800 TC cycles.[30] Along with the TC tests, one shingled full-size module with SHJ cells was submitted to sequential tests at PI Berlin. These tests included LID (light-induced degradation) (2× 5 kWh/m^2, E_e = 1000 W/m^2; T_{mod} = 50°C, MPP-Mode) followed by LeTID (Light and elevated Temperature Induced Degradation) (214 h, 75°C, 2× Isc – Imax) and PID (Potential-Induced Degradation)

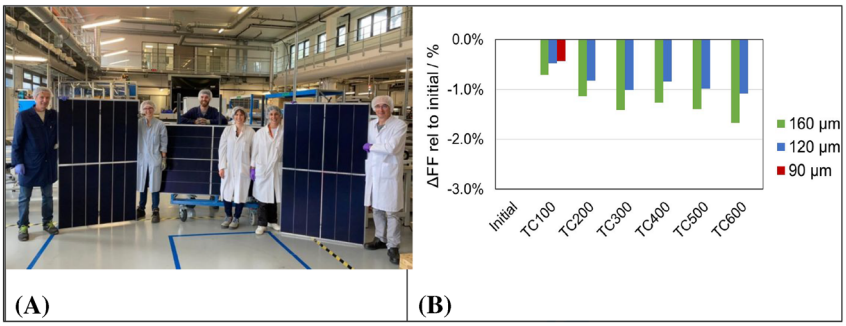

FIGURE 11 (A) 60-M2 cell equivalent SHJ shingled modules using 12 strings of 32 cut-cells and a glass–glass design. *Source*: CEA. (B) Evolution of ΔFF after TC for SHJ shingle modules integrating different wafer thicknesses; 90 µm configuration is currently still going through further extensive TC tests. *Source*: CEA[31] [Colour figure can be viewed at wileyonlinelibrary.com]

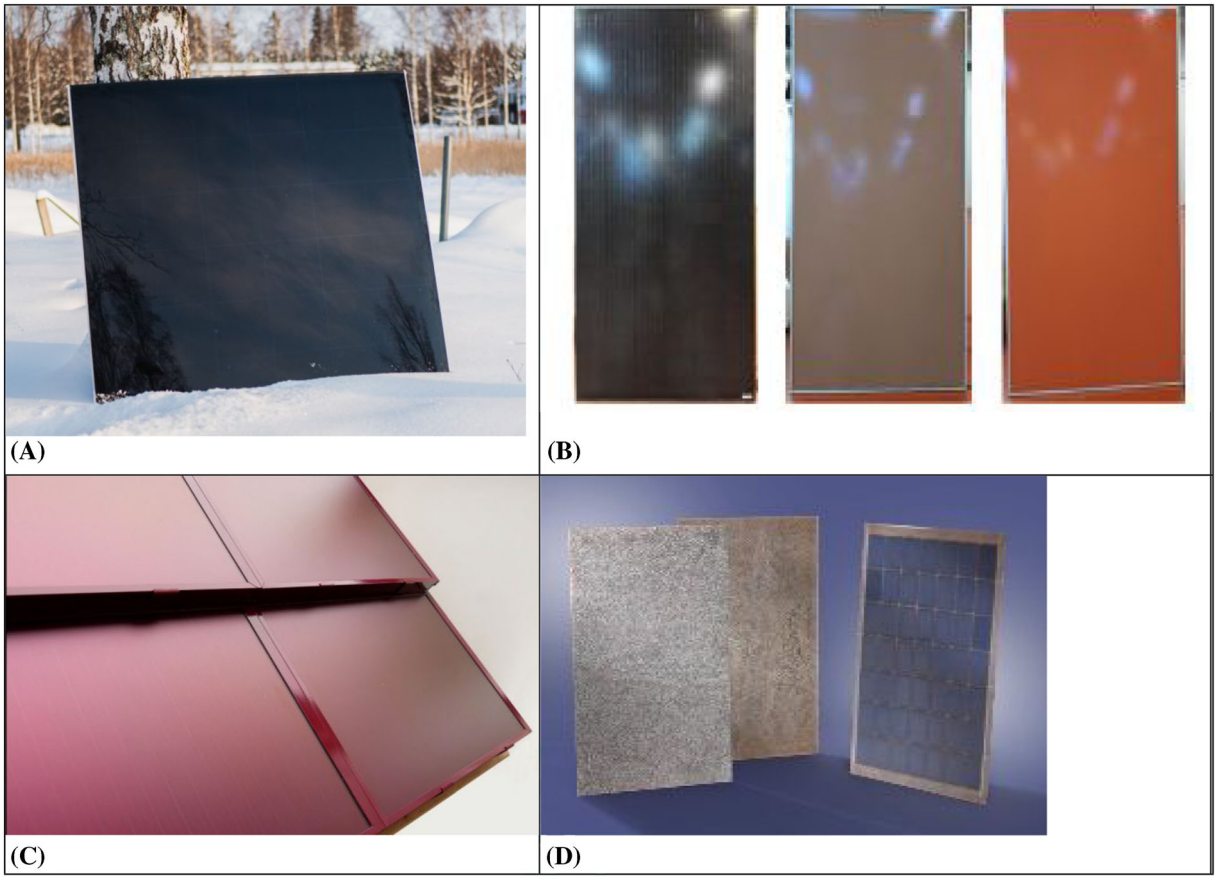

FIGURE 12 (A) Lightweight BIPV module with IBC cells. *Source*: Valoe Oyj. (B) Colored SHJ shingled module with black, brown, or orange intercalation foils for BIPV application. *Source*: Voltec Solar. (C) Colored BIPV module using shingling and Morphocolor™ technologies. *Source*: Fraunhofer ISE.[54] (D) BIPV modules with a thin stone veneer on the front side. *Source*: ISFH[55] [Colour figure can be viewed at wileyonlinelibrary.com]

sensitivity test (1000 V, 85°C, 85% RH with 12 h DH preconditioning) with positive and negative bias. The module showed no apparent degradation in P_{max} after LID, LeTID, and PID(+) while P_{max} degradation after PID(−) stayed below $2\%_{rel.}$ indicating further room for improvement.

Further experiments were then initiated to optimize the cost of SHJ shingled modules following different paths. The first path focused on the reduction of the overall Ag usage in the shingle process (pattern optimization, ECA with reduced Ag content, etc.). While ECA consumption in the previous tests was about 3–4 mg per shingle, the goal was to lower the consumption down to <1 mg per shingle mainly by reducing the number and size of the ECA pads. Characterization on small modules showed no significant impact on either initial performance or reliability with <2% loss in P_{max} after 600TC.[30] The second path focused on the qualification of the process with thin wafers (160 µm down to 90 µm) to further reduce the carbon footprint of PV modules.[31] Several SHJ shingle strings with, respectively, 90 µm, 120 µm, and 160 µm thick cells were assembled and manufactured into modules and subjected to TC testing. Initial module performances indicate no loss of power when moving from 160 µm to 120 µm. For

90 µm cells, initial module performances are slightly degraded, linked to the lower power of thin cells as they become more sensitive to damages during cell processing. However, in terms of reliability, modules with thinner cells (90 or 120 µm) seem to benefit from the absence of ribbons, which can generate cracks on the wafers, and TC resistance of the shingle interconnection is facilitated by the increased mechanical flexibility of the thin wafers (see Figure 11B).

3.7 | Tailored PV module design for BIPV

In HighLite module manufacturers supported by several research organizations targeted specific features for BIPV modules (see examples in Figure 12). Valoe realized a demonstrator showing a power density of 200 Wp/m^2 and a specific weight of 5.3 kg/m^2 with a smart junction box integrating a maximum power point (MPP) tracker. These modules are destined to be used for balconies and other applications requiring lightweight (e.g., PV on light and heavy commercial vehicles). Voltec produced lightweight BIPV module prototypes with a uniform all-black appearance using SHJ shingled strings assembled by AMAT (see Figure 8B). Further optimization is on-going to obtain full area module efficiencies above 21%. Voltec, Fraunhofer ISE, and CSEM also built shingled SHJ colored modules with monochromatic orange or brown laminated foils showing, respectively, 25% and 66% lower efficiencies compared with the all-black reference. The colored foils showed no impact on reliability tests such as DH, TC and UV tests. Fraunhofer ISE realized a demonstrator roof element comprising 6 tile modules using its Morphocolor™ technology[54] and matching colored Al frames. ISFH demonstrated the feasibility of making BIPV modules with a thin stone layer on the front side, that are to be used as façade elements. This stone veneering natural surface roughness combined with its colorful pattern provides the illusion of a massive stone building element. As it can expected, the application of stone veneers leads to efficiencies losses in the range of 50% compared with a typical all-black BIPV product which is still very interesting for architects looking to replace passive stone claddings.[55] Altogether, these developments are important to increase the design freedom for architects to realize nearly zero energy buildings (NZEB) or houses and even positive energy districts (PED) in the near future.

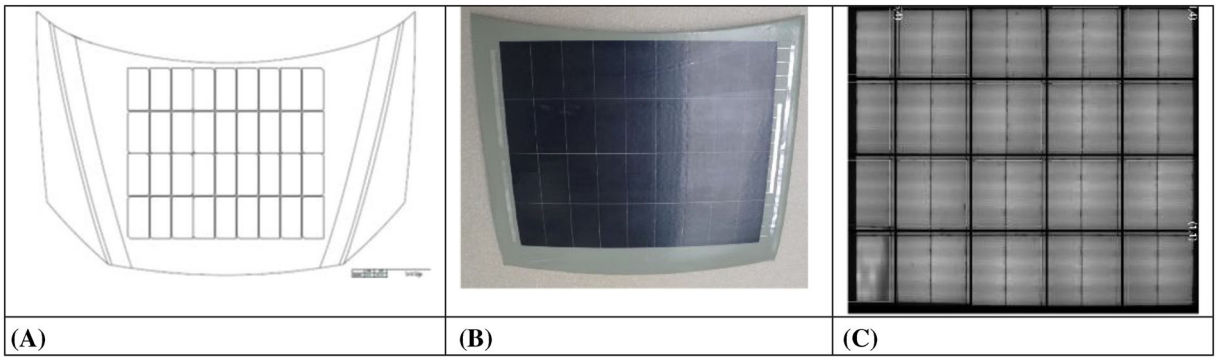

FIGURE 13 (A) Layout of the IBC cut cells on the VIPV demonstrator car bonnet, (B) picture of reduced-size VIPV module, and (C) electroluminescence (EL) image of the VW Polo VIPV demonstrator taken after lamination and before the vibration testing. *Source*: ISFH [Colour figure can be viewed at wileyonlinelibrary.com]

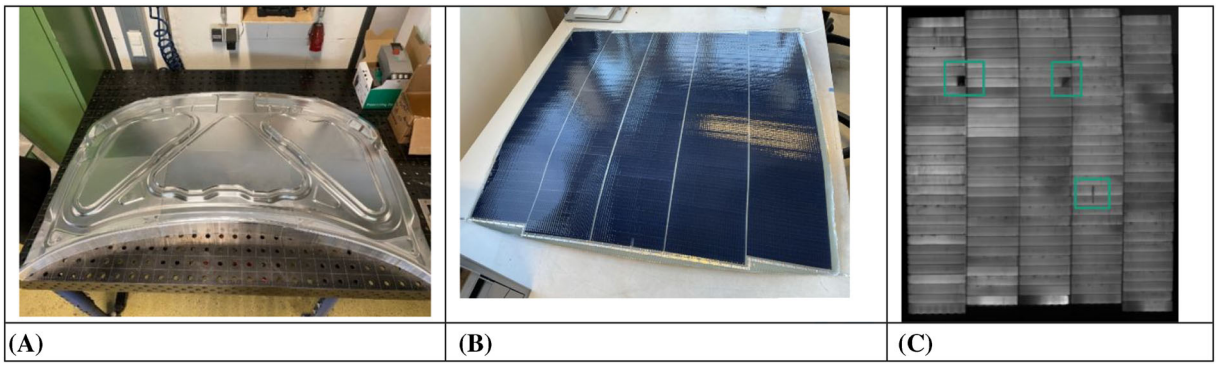

FIGURE 14 (A) Aluminum form for the lamination process, (B) picture of a reduced-size VIPV module with five shingle string, and (C) electroluminescence (EL) image of the VIPV module after lamination, before the vibration testing [Colour figure can be viewed at wileyonlinelibrary.com]

3.8 | Tailored PV module designs for VIPV

The main goal here is develop 3D curved lightweight PV modules with improved efficiency, uniform optical appearance, and advanced reliability (in particular resilience against vibrations) for passenger cars. For this purpose, several Volkswagen Polo car bonnets were acquired. After optimizing the different cell technologies, bill of materials, lamination systems, and processes, three different types of VIPV modules were produced by the HighLite partners.

The VIPV module from ISFH was manufactured using a double membrane laminator with a flexible heating element enclosed between two airtight silicone membranes. The module was made with ZEBRA IBC cells provided by ISC Konstanz and interconnected with soldered ribbons. The chosen layout comprises 36 half cells connected in a 4 × 9 matrix as shown in Figure 13A. As the demonstrator module is destined to be submitted to vibration testing on a shaker with limited area, the cells were laminated on a cut-out of the bonnet. The Figure 13B shows a picture of the car bonnet after lamination as well as an electroluminescence (EL) image (cf. Figure 13C) showing that no cell breakage occurred during the lamination of the cells on the 3D curved surface of the car bonnet.

Another 3D curved VIPV module was realized at Fraunhofer ISE using single membrane lamination. This required using a dedicated negative form in Aluminum (Al), see Figure 14A, which has a thermal conductivity between 110–130 W/(m*K). Because of the partially hollow structure of the backside of the bonnet it was mandatory to optimize the temperature distribution on the surface of the bonnet during the lamination process. The optimized module area on the bonnets was calculated for strings with TOPCon shingle cells obtained from G1 wafers.[56] For each string, 30 shingle cells were used and for one bonnet, five strings were interconnected in parallel. From the EL images (cf. Figure 14C) it is visible, that only a few minor defects occurred during the lamination process.

A further VIPV module was developed at IMEC. Imec has been developing approaches where (mostly glass-fiber-based) reinforcement is applied in the polymer encapsulant and/or back cover in order to reach a weight <5 kg/m^2. With promising results in terms of thermal cycling and damp heat exposure, as well as hail impact and vibration testing, the next step was to apply this for a VIPV application. After successful pre-tests, the lamination was performed in a double-membrane laminator at IMEC. For the layout four strings of 30 shingle SHJ cells were used. To avoid wrinkling issues, a layup without full layers of front- and backsheet was done. In this case, the total weight is slightly lower at 2.20 kg (absolute) or 3.9 kg/m^2 due to the absence of the frontsheet. While this is a promising result, it is not the final solution. As work in progress, the next steps are to look into either plastically deforming the frontsheet material, or using preformed frontsheets, potentially combined with stretchable materials.[57]

After manufacturing all VIPV modules were I-V (and EL) measured at IMEC, prior the vibration tests. From Figure 15, it is visible, that all

Isc [A]	Voc [V]	FF [%]	Vmpp [V]	Impp [A]	Pmpp [W]	
5.687	22.090	78.3	18.066	5.447	98.403	IMEC
Isc [A]	Voc [V]	FF [%]	Vmpp [V]	Impp [A]	Pmpp [W]	
4.927	24.830	79.7	20.880	4.671	97.539	ISFH
Isc [A]	Voc [V]	FF [%]	Vmpp [V]	Impp [A]	Pmpp [W]	
7.814	20.867	79.2	17.404	7.421	129.151	F-ISE

FIGURE 15 IV results for the VIPV modules from IMEC, ISFH, and F-ISE [Colour figure can be viewed at wileyonlinelibrary.com]

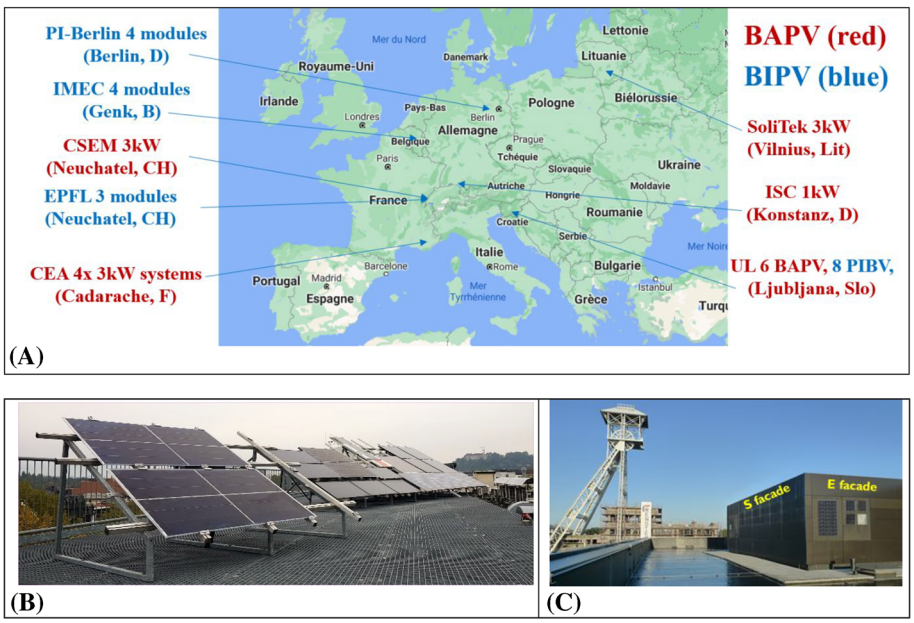

FIGURE 16 (A) List of sites for outdoor monitoring of BABV (red) and BIPV (blue) modules. (B) BAPV monitoring site at University of Ljubljana (UL) in Slovenia (azimuth: south, tilt: 30°). (C) BIPV monitoring site at imec in Genk in Belgium (azimuth: south and east, tilt: 90°) [Colour figure can be viewed at wileyonlinelibrary.com]

VIPV modules reached fill factors between 78.3–79.7%, independent of the module layout. Vibration testing of those demo VIPV modules equivalent to 1000 km of driving has now been started and results will be reported elsewhere.

3.9 | Outdoor testing results

A total of more than 60 BAPV and BIPV demonstrator modules have been fabricated, characterized, installed, and monitored together with 26 representative benchmark modules. Eight partners are monitoring at their site located across Europe and using either open racks or facade integration (see Figure 16). The sites are located from North to South, at Solitek in Vilnius (Lithuania), imec in Genk (Belgium), PI-Berlin (Germany), ISC-Konstanz (Germany), CSEM/EPFL in Neuchatel (Switzerland), University of Ljubljana (Slovenia), and CEA in Cadarache (France). Four strings of five modules are monitored using the standard IEC 61724-1,[58] while the rest is monitored individually giving a high granularity of the data. Grouping the data on a shared online monitoring platform (in-house developed) allowed to have the same

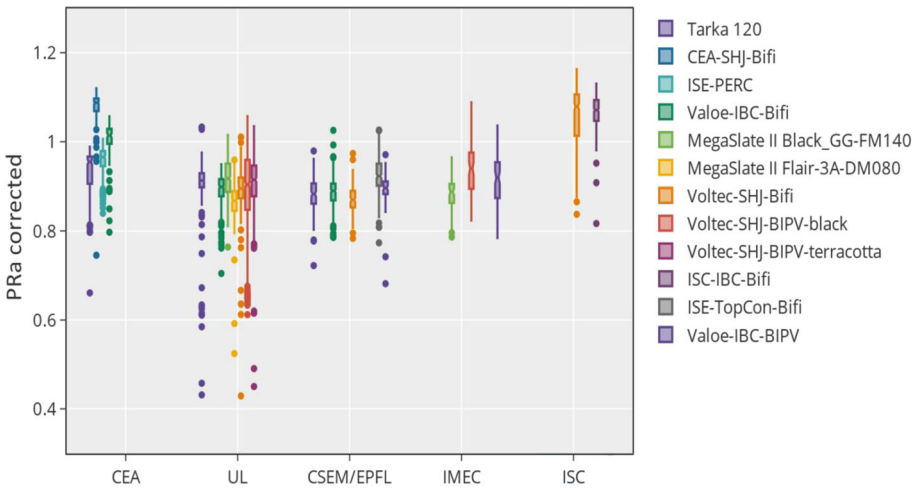

FIGURE 17 Box-plot of the monthly performance ratio of the array corrected for temperature (PRa_corrected or PRa_corr in short) for the different module types and locations [Colour figure can be viewed at wileyonlinelibrary.com]

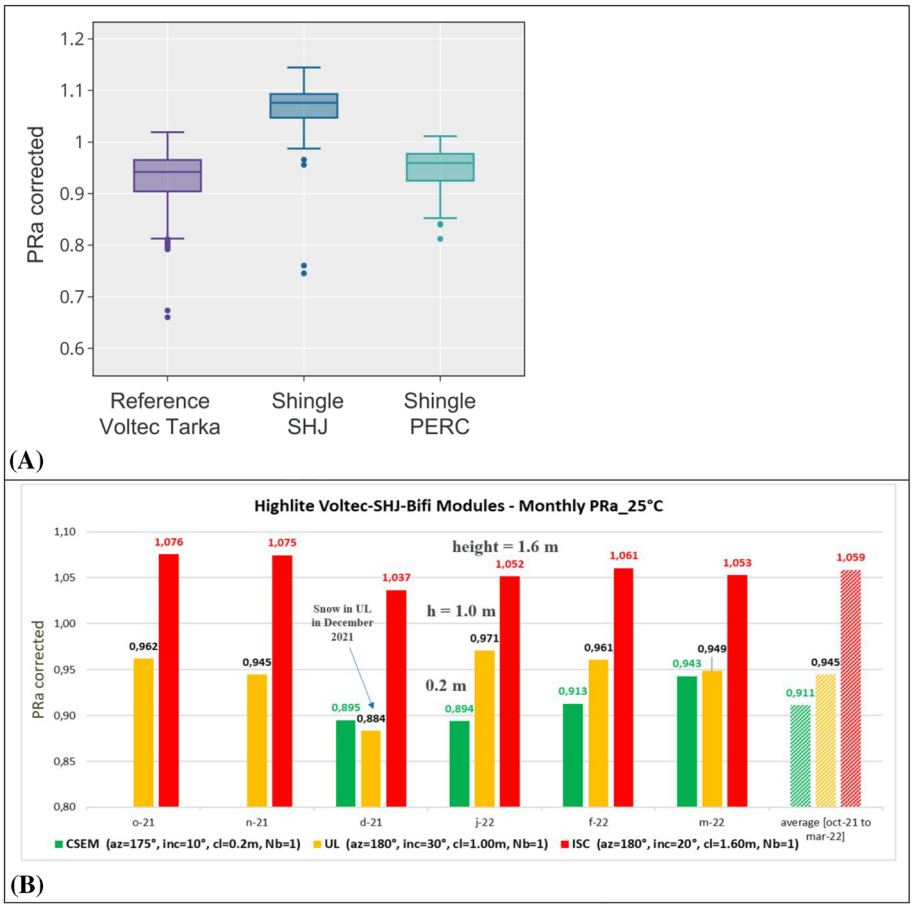

FIGURE 18 (A) Average PRa corrected for temperature for systems installed at CEA in Cadarache. (B) Monthly PRa corrected for temperature for shingle SHJ bifacial module installed in CSEM/EPFL, UL, and ISC [Colour figure can be viewed at wileyonlinelibrary.com]

data treatment to avoid errors and to plot all the data together for easier interpretation of the results (see Figure 17).

In Figure 18A, the average performance ratio corrected by the temperature (PRa_corr) is plotted for three different module types installed at CEA in Cadarache. The benchmark module is the "Voltec-Tarka" based on 120 half-cut 9BB PERC cells and glass-backsheet (GBS); the second module type called "Shingle SHJ" is based on bifacial SHJ shingles in glass–glass (GG) configuration; and the final configuration called "Shingle PERC" is based on monofacial PERC shingles in GG configuration. The PRa_corr changes from 0.94, 0.96, to 1.08 for the Tarka, Shingle PERC, and Shingle SHJ, respectively. We can see that the effect of changing from half-cut 9BB PERC in GBS to shingle PERC in GG does not change drastically the PRa_corr (+2%), whereas to change from monofacial shingle PERC to bifacial shingle SHJ cells improved the PRa_corr by +12.5%. This gain is in the same order but slightly lower than the simulated value proposed by Shoukry et al.[59] for similar operating conditions (albedo = 0.3, module height = 1.5 m).

The elevation of the bifacial modules is improving their gain versus mono-facial module as shown in Figure 18B. The module elevations are 0.2, 1.0, and 1.6 m high for CSEM/EPFL, UL, and ISC, respectively. Over the period from October 2021 to March 2022, the PRa_corr is +3.4% from 0.2 m to 1.0 m and +12.3% from 1.0 m to 1.6 m, instead the gain should be higher from 0.2 m to 1.0 m according to literature.[60] One hypothesis is the prolonged presence of snow load in UL during December 2021 which reduced the PRa_corr compared with other sites.

The morning and evening PRa_corr can be strongly influenced by the position of the reference cells (or pyranometer) as shown in Figure 19 bottom. From May 8 to 17, a first reference cell is used and the PRa_corr over time shows a square shape and the PRa_corr versus irradiance plot shows a low value at low irradiance (possibly partial shadowing of the string at sunrise and/or sunset). By changing the reference cell after May 19, the behavior at sunrise and sunset changes drastically, showing spikes of PRa_corr in the morning and in the evening, possibly due to under-estimation of the irradiance by the new reference cell. This effect is well shown on the graph of PRa_corr versus irradiance (Figure 19 top). Introducing a threshold in the data with irradiance <50 W/m^2 (as shown by the gray squares in the graphs and proposed in the IEC 61724-1[58]), the influence of the positing of the reference cell (or pyranometer) will not be observed in the monthly PRa_corr value.

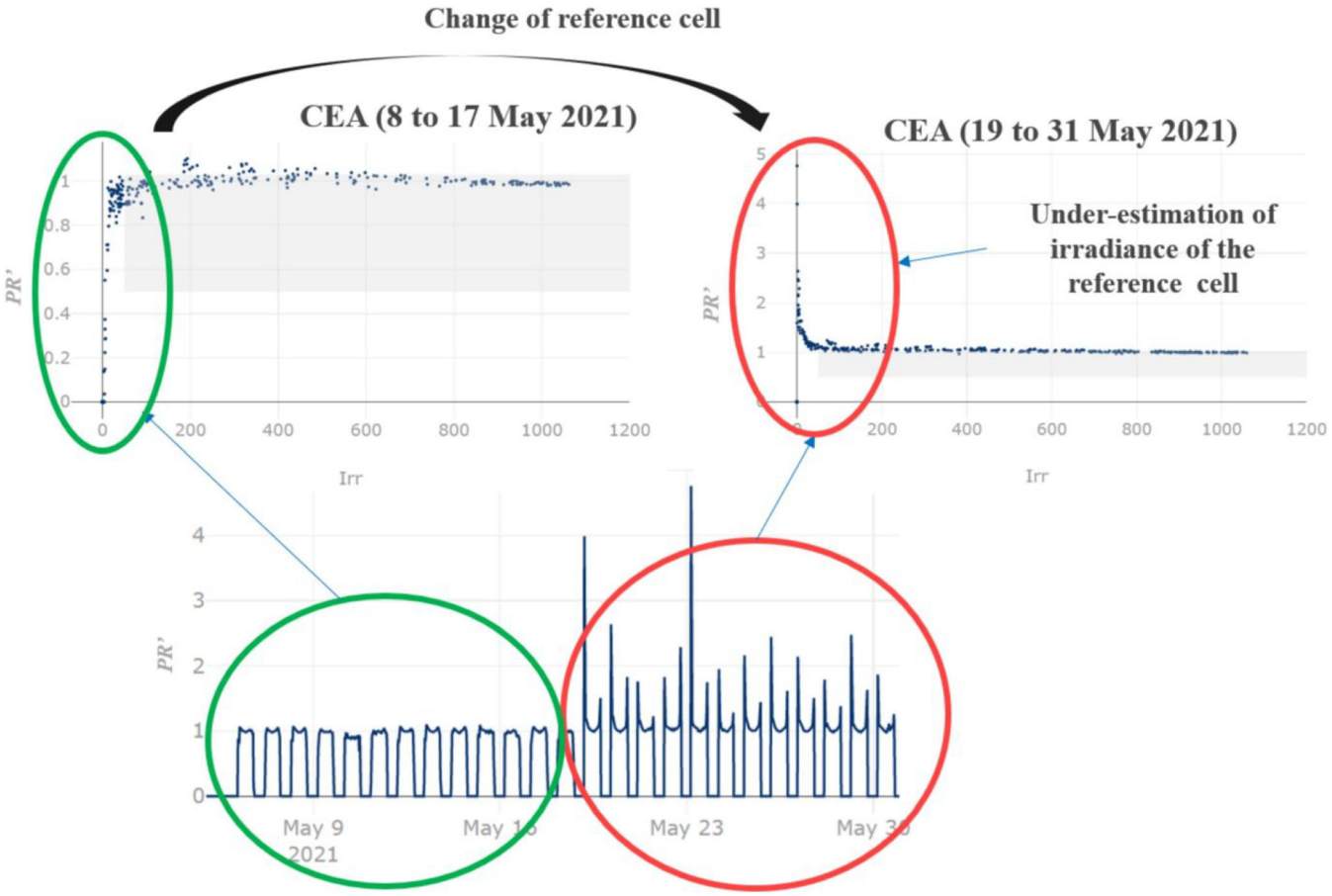

FIGURE 19 Top graphs: PRa corrected by temperature versus irradiance for the string of 10 benchmark modules Tarka-120 measured in Cadarache, bottom graph: PRa corrected by temperature between May 8 and 31, 2021 [Colour figure can be viewed at wileyonlinelibrary.com]

3.10 | Life cycle analysis

The HighLite project has ambitious goals on reducing the environmental impact of the module technologies developed. One of the final goals of the project due in March 2023 is to manufacture a BAPV module with >22% efficiency and a carbon footprint of 250 kg-eq. CO_2/kWp. The section briefly shows what is needed for this goal to be achieved.

To this end, a reference PV module is defined representing state-of-the-art PV technology. The life-cycle inventory data required to calculate a breakdown of the carbon footprint of this reference were assembled using data published by the IEA PVPS Task 12 group.[61] The calculations were carried out using the commercial LCA software Simapro in conjunction with the Ecoinvent database. A (module level) carbon footprint of 1120 kg CO2-eq./kWp was found.

Based on this reference value, a systematic analysis of carbon footprint reduction potentials was carried out. The focus of this analysis was on reduction potentials arising from specific goals of the HighLite project, such as 22% PV module efficiency as well as the implementation of thin wafers down to 100 µm and frameless glass/glass module configuration. With these innovations significant carbon footprint reductions on the order of ~25% can be expected. These innovations alone will not suffice to reach the carbon footprint goal of the HighLite project. Therefore, other additional potentials to reduce the carbon footprint were also analyzed. This analysis reveals that the use of "green electricity" with very low inherent carbon footprint (such as hydropower) is pivotal to achieve further large reductions of the carbon footprint. When implementing this type of "green electricity" throughout the entire PV value chain, further carbon footprint reduction by as much as ~60% can be achieved. In combination with the use of green electricity the innovations of the HighLite project will make the carbon footprint goal of 250 kg-eq.CO_2/kWp achievable, as can be seen in Figure 20.

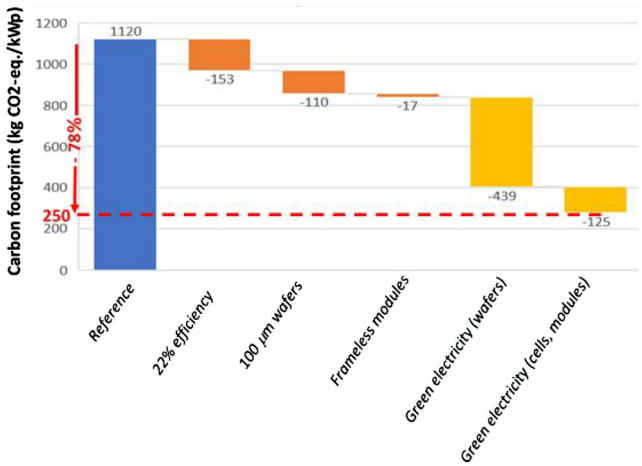

FIGURE 20 Waterfall chart showing carbon footprint potentials associated with the HighLite project goals (orange) as well as other potentials (yellow) [Colour figure can be viewed at wileyonlinelibrary.com]

4 | SUMMARY AND CONCLUSIONS

As discussed in the introduction section, the EU PV manufacturing industry needs to focus on highly performing c-Si PV technologies, include sustainability by design, and develop differentiated PV module designs for a broad range of PV applications to tap into rapidly growing existing and new markets as well as differentiate itself from the foreign competition. In this context and to improve the competitiveness of the EU PV manufacturing industry, the HighLite project has been focusing since its inception in 2019 on bringing advanced module designs based on SHJ shingle and IBC cut-cells to higher technology readiness levels (TRL). Both technologies have the potential to significantly outperform mainstream products based on PERC technology in terms of performance, aesthetics, modularity, and sustainability. Key results obtained by the project partners include various innovations at cell and module levels as well as improved understanding of cut edge recombination losses and the pathways needed to drastically reduce the carbon footprint of PV modules manufactured in EU. In detail, the partners demonstrated highly efficient and low-cost industrial SHJ shingle and IBC cells (up to 24.1% and 23.9%, respectively), novel approaches and equipment to minimize cut-edge recombination losses, highly flexible and automated equipment for the assembly of cut cells, and tailored PV module designs for various applications including BAPV, BIPV, and VIPV. Several of those innovations go well beyond the current state-of-the-art and are generic enough to benefit other c-Si PV module designs. For example, the approaches and related equipment/characterization techniques developed for advanced cutting and edge re-passivation are applicable not only to the n-type concepts (SHJ and IBC) studied in HighLite but also to other cell concepts (PERC, MWT, TOPCON). Similarly, the efforts made to improve sustainability/durability/eco-design (reduced Si and Ag consumption per Wp, lead-free interconnection, steps needed to achieve carbon footprint <250 kg CO_2-eq./kWp, etc.) are relevant for multiple PV module designs and are in line with future eco-design directives at EU level. Finally, with buildings responsible for 36% of energy-related greenhouse gas emissions in the EU and transport accounting for another 30%, the developments made in HighLite to tailor PV module designs specifically for BIPV and VIPV applications are highly relevant to support the expected rapid growth of those applications in the near future.

AFFILIATIONS

[1]imec, imo-imomec, Genk, Belgium
[2]Hasselt University, imo-imomec, Hasselt, Belgium
[3]EnergyVille, imo-imomec, Genk, Belgium
[4]CEA, CEA-LITEN, INES, Le Bourget-du-Lac, France
[5]ISC Konstanz, Konstanz, Germany
[6]CSEM, Neuchâtel, Switzerland
[7]EPFL, Lausanne, Switzerland
[8]Fraunhofer ISE, Freiburg im Breisgau, Germany
[9]ISFH, Emmerthal, Germany
[10]University of Ljubljana, Ljubljana, Slovenia
[11]TNO, Energy Transition – Solar Energy, Petten, Netherlands

[12]PI Berlin, Berlin, Germany
[13]Applied Materials, Olmi, Italy
[14]Henkel, Westerlo, Belgium
[15]Ion Beam Services IBS, Peynier, France
[16]3D-Micromac, Chemnitz, Germany
[17]SoliTek, Vilnius, Lithuania
[18]Valoe Cells UAB, Vilnius, Lithuania
[19]Valoe Oyj, Mikkeli, Finland
[20]Voltec Solar, Dinsheim-sur-Bruche, France
[21]TU Delft, Delft, Netherlands

ACKNOWLEDGMENT

This project has received funding from the European Union's Horizon 2020 Programme for research, technological development, and demonstration under Grant Agreement no. 857793.

DATA AVAILABILITY STATEMENT

Research data are not shared.

ORCID

Loic Tous https://orcid.org/0000-0001-9928-7774
Valentin Giglia https://orcid.org/0000-0003-4239-2332
Antonin Faes https://orcid.org/0000-0001-7871-2559
Hugo Quest https://orcid.org/0000-0003-3945-3093
Florian Schindler https://orcid.org/0000-0001-7639-2758
Miha Kikelj https://orcid.org/0000-0002-1591-2585
Marko Topic https://orcid.org/0000-0001-8089-2974
Tadas Radavicius https://orcid.org/0000-0002-5222-7499

REFERENCES

1. SolarPower Europe. EU market outlook for solar power 2021–2025. 2021. ISBN: 9789464444292.
2. Heiber J, Bloch R, Bucher R, et al. A review of diamond wire wafering technology at Meyer Burger Ltd. In: Reddig K, ed. *Manufacturing the Solar Future: The 2011 Production Annual*. Solar Media:78-85.
3. Kerschaver EV, Beaucarne G. Back-contact solar cells: a review. *Prog Photovolt: Res Appl*. 2006;14(2):107-123. doi:10.1002/pip.657
4. Dullweber T, Kranz C, Peibst R, et al. PERC+: industrial PERC solar cells with rear Al grid enabling bifaciality and reduced Al paste consumption. *Prog Photovolt: Res Appl*. 2016;24(12):1487-1498. doi:10.1002/pip.2712
5. Galbaiti G, Mihailetchi VD, Halm A, Chu H, Kopecek R. "Large area IBC ZEBRA solar cells in pilot production: the results of FP7 HERCULES project.", in Proceedings of the 32nd EUPVSEC. 2016:980–982.
6. Preu R, Lohmüller E, Lohmüller S, Saint-Cast P, Greulich JM. Passivated emitter and rear cell—devices, technology, and modeling. *Appl Phys Rev*. 2020;7(4):041315. doi:10.1063/5.0005090
7. Hermle M, Feldmann F, Bivour M, Goldschmidt JC, Glunz SW. Passivating contacts and tandem concepts: approaches for the highest silicon-based solar cell efficiencies. *Appl Phys Rev*. 2020;7(2):021305. doi:10.1063/1.5139202
8. Ballif C, Haug FJ, Boccard M, Verlinden PJ, Hahn G. Status and perspectives of crystalline silicon photovoltaics in research and industry. *Nat Rev Mater*. 2022;1-20.
9. Bennett IJ, Janssen RH, van Duijnhoven F, Xu J. "Development of conductive back-sheet for manufacture of PV modules with back-contact cells." 2018 IEEE 7th World Conference on Photovoltaic Energy Conversion (WCPEC). 2018:3623–3625.
10. Braun S, Hahn G, Nissler R, Pönisch C, Habermann D. The multi-busbar design: an overview. *Energy Procedia*. 2013;43:86-92. doi:10.1016/j.egypro.2013.11.092
11. Papet P, Andreetta L, Lachenal D, et al. New cell metallization patterns for heterojunction solar cells interconnected by the smart wire connection technology. *Energy Procedia*. 2015;67:203-209. doi:10.1016/j.egypro.2015.03.039
12. Klasen N, Weisser D, Rößler T, Neuhaus DH, Kraft A. Performance of shingled solar modules under partial shading. *Prog Photovolt: Res Appl*. 2022;30(4):325-338. doi:10.1002/pip.3486
13. Dullweber T, Tous L. *Silicon Solar Cell Metallization and Module Technology*. The Institution of Engineering and Technology. ISBN-13: 978-1-83953-155-2.
14. Chen Y, Altermatt PP, Chen D, et al. From laboratory to production: learning models of efficiency and manufacturing cost of industrial crystalline silicon and thin-film photovoltaic technologies. *IEEE J Photovolt*. 2018;8(6):1531-1538. doi:10.1109/JPHOTOV.2018.2871858
15. SolarPower Europe. Global market outlook for solar power 2022–2026. 2022. ISBN: 9789464518610.
16. Colletti C, Gerardi C, Bizzarri F, et al. "AMPERE: the European PV manufacturing ready to compete in the premium high efficiency market". in Proceedings of the 37th EUPVSEC. 2020:256–260.
17. SolarPower Europe. Putting solar in the driver's seat solar mobility report. 2019. ISBN: 9789463965903.
18. Polverini D, Dodd N, Espinosa N. Potential regulatory approaches on the environmental impacts of photovoltaics: expected improvements and impacts on technological innovation. *Prog Photovolt: Res Appl*. 2021;29(1):83-97. doi:10.1002/pip.3344
19. Müller A, Friedrich L, Reichel C, Herceg S, Mittag M, Neuhaus DH. A comparative life cycle assessment of silicon PV modules: impact of module design, manufacturing location and inventory. *Sol Energy Mater sol Cells*. 2021;230:111277. doi:10.1016/j.solmat.2021.111277
20. Green MA, Dunlop ED, Hohl-Ebinger J, et al. Solar cell efficiency tables (version 60). *Prog Photovolt: Res Appl*. 2022;30(7):687-701. doi:10.1002/pip.3595
21. Giglia V, Veirman J, Varache R, Portaluppi B, Harrison S, Fourmond E. "Influence of edge recombinations on the performance of half-, shingled-and full silicon heterojunction solar cells." in Proceedings of the 37th EUPVSEC. 2020:282–285.
22. Baliozian P, al-Akash M, Lohmuller E, et al. Post metallization "passivated edge technology" for separated silicon solar cells. *IEEE J Photovolt*. 2020;10(2):390-397. doi:10.1109/JPHOTOV.2019.2959946
23. Kopecek R, Libal J, Lossen J, et al. "ZEBRA technology: low cost bifacial IBC solar cells in mass production with efficiency exceeding 23.5%" In Proceedings of the 47th IEEE Photovoltaic Specialists Conference (PVSC). 2020:1008–1012.
24. Buchholz F, Linke J, Hoß J, et al. "Local passivating contacts from laser doped P+ polysilicon." in Proceedings of the 38th EUPVSEC. 2021:140–143.
25. Haase F, Hollemann C, Schafer S, Krügener J, Brendel R, Peibst R. "Transferring the record p-type Si POLO-IBC cell technology towards an industrial level." In Proceedings of the 46th IEEE Photovoltaic Specialists Conference (PVSC). 2019:2200–2206.
26. Touloupas G, Kearns-McGay C. "New technologies, new risks: edge ribbon cracking", PV magazine. April 2022 edition, pp. 54–55.
27. Baliozian P, Munzer A, Lohmuller E, et al. Thermal laser separation of PERC and SHJ solar cells. *IEEE J Photovolt*. 2021;11(2):259-267. doi:10.1109/JPHOTOV.2020.3041251
28. Kroon JM, Newman BR, Govaerts J, Voroshazi E, Borgers T. Advances in module interconnection technologies for crystalline silicon solar cells. *Photovolt Int*. 2018;41:93-107.
29. Giglia V, Varache R, Veirman J, Fourmond E. Understanding of the influence of localized surface defectivity properties on the

performances of silicon heterojunction cells. *Prog Photovolt: Res Appl*. 2020;28(12):1333-1344. doi:10.1002/pip.3330
30. Carrière C, Barth V, Harrison S, et al. "Shingle interconnection on HJT solar cells: reliability study and upscaling for high power PV modules." in Proceedings of the 38th EUPVSEC, 2021.
31. Carrière C, Harrison S, Barth V, et al. "Pushing the limits of heterojunction shingle modules performance, cost and sustainability", in Proceedings of the 8th WCPEC, 2022.
32. Zhang Y, Kim M, Wang L, Verlinden P, Hallam B. Design considerations for multi-terawatt scale manufacturing of existing and future photovoltaic technologies: challenges and opportunities related to silver, indium and bismuth consumption. *Energ Environ Sci*. 2021;14(11):5587-5610. doi:10.1039/D1EE01814K
33. Harrison S, Barth V, Carrière C, et al. "Simplified cell cutting, efficient edge passivation, copper metallization: tackling the last hurdles for optimized SHJ integration in Shingle module configuration", in *Proceedings of the 8th WCPEC*, 2022.
34. Fellmeth T, Feldmann F, Steinhauser B, et al. "A round robin—HighLiting on the passivating contact technology." in Proceedings of the 38th EUPVSEC, pp. 181–185, 2021.
35. Fırat M, Wouters L, Lagrain P, et al. Local enhancement of dopant diffusion from polycrystalline silicon passivating contacts. *ACS Appl Mater Interfaces*. 2022;14(15):17975-17986. doi:10.1021/acsami.2c01801
36. Kafle B, Goraya BS, Mack S, Feldmann F, Nold S, Rentsch J. TOPCon–technology options for cost efficient industrial manufacturing. *Sol Energy Mater sol Cells*. 2021;227:111100. doi:10.1016/j.solmat.2021.111100
37. Min B, Wehmeier N, Schulte-Huxel H. "Approaching 23% with p-type back junction solar cells featuring screen-printed Al front grid and passivating rear contacts." in Proceedings of the 38th EUPVSEC. 2021:158–161.
38. Desrues T, Oliveau C, Seron C. "Doping and hydrogenation processes for passivating contact solar cells using plasma immersion ion implantation (PIII)." in Proceedings of the 37h EUPVSEC. 2020:173–175.
39. Haug F-J, Morisset A, Wyss P, et al. Passivating polysilicon recombination junctions for crystalline silicon solar cells. *Phys Status Solidi - Rapid Res Lett*. 2021;15(9):2100272. doi:10.1002/pssr.202100272
40. Bokalic M, Kikelj M, Lipovsek B, Harrison S, Topic M. Insights into cut-edges of SHJ solar cells by EL and LBIC characterization 2022.
41. Bokalic M, Kikelj M, Brecl K, et al. "EL and LBIC characterization of cut edge recombination in IBC solar cells." In Proceedings of the 37th EUPVSEC, pp. 308–311. doi:10.4229/EUPVSEC20202020-2CV.1.9
42. Kikelj M, Lipovšek B, Bokalič M, Buchholz F, Topič M. "Detailed 3D optical modelling of interdigitated back contact solar cells." in Proceedings of the 48th *IEEE PVSC*, pp. 0997–1000. doi:10.1109/PVSC43889.2021.9518850
43. Kikelj M, Lipovšek B, Bokalič M, Buchholz F, Topič M. "Do not blame the butter for what the bread did" or how the optical properties of IBC solar cells affect the results of spatially resolved characterization methods. in Proceedings of the 38th EUPVSEC, pp. 229–232. doi:10.4229/EUPVSEC20212021-2CV.1.4
44. Kikelj M, Bokalič M, Topič M, Lipovšek B. Detailed luminescence modelling in high-efficiency solar cells for precise calibration of spatially resolved characterisation methods: a bottom-up opto-electrical. *Under Rev*. 2022;248:111990. doi:10.1016/j.solmat.2022.111990
45. Stolzenburg H, Fell A, Schindler F, et al. Edge recombination analysis of silicon solar cells using photoluminescence measurements. *AIP Conf Proc*. 2019;2147:020017. doi:10.1063/1.5123822
46. Chen N, Tune D, Buchholz F, Halm A, Mihailetchi VD. "Impact of cut edge recombination in high efficiency solar cells—measurement and mitigation strategies." in Proceedings of the 38th EUPVSEC, pp. 253–256. doi:10.4229/EUPVSEC20212021-2CV.1.12
47. Münzer A, Baliozian P, Steinmetz A, et al. Post-separation processing for silicon heterojunction half solar cells with passivated edges. *IEEE J Photovolt*. 2021;11(6):1343-1349. doi:10.1109/JPHOTOV.2021.3099732
48. Harrison S, Portaluppi B, Bertrand P, et al. "Low temperature post-process repassivation for heterojunction cut-cells." in Proceedings of the 38th EUPVSEC. 2021:167–171.
49. Chen N, Buchholz F, Tune D, Halm A, Isabella O, Mihailetchi V. "Reducing cut losses of interdigitated back-contact solar cells", To be published in Proceedings of the WCPEC 8. 2022.
50. Chen N, Buchholz F, Tune DD, Isabella O, Mihailetchi VD. Mitigating cut losses in interdigitated back contact solar cells. *IEEE J Photovolt*. 2022;12(6):1386-1392. doi:10.1109/JPHOTOV.2022.3208507
51. Zhang C, Shen H, Liu H, Zhang W, Chen J, Li H. Influence of laser condition on the electrical and mechanical performance of bifacial half-cutting PERC solar cell and module. *Int J Energy res*. 2022;46(11):15290-15299. doi:10.1002/er.8229
52. Halm A. "Achieving uniform module appearance while increasing module efficiency: the full gapless module concept for stringed IBC solar cells", To be published in Proceedings of the WCPEC 8. 2022.
53. Tummalieh A, Paritala B, Mittag M, Neuhaus DH. "Interconnection Technology in PV Modules: Impact of Ribbons, Tab Connectors and Electrically Conductive Backsheet on Module Performance." To be published in Proceedings of the WCPEC 8. 2022.
54. Bläsi B, Kroyer T, Kuhn TE, Höhn O. The MorphoColor concept for colored photovoltaic modules. *IEEE J Photovolt*. 2021;11(5):1305-1311. doi:10.1109/JPHOTOV.2021.3090158
55. Morlier A, Lim B, Blankemeyer S, et al. Photovoltaic modules with the look and feel of a stone facade for building integration. *Solar RRL*. 2021;6(5):2100356. doi:10.1002/solr.202100356
56. Nikitina V, Reinwand D, Fellmeth T, et al. "Application of SHJ and TOPCon shingle cells in full-format and integrated solar modules", To be published in Proceedings of the WCPEC 8. 2022.
57. Govaerts J, van der Heide A, Van Dyck R, et al. "Interconnection and lamination technologies towards ubiquitous PV technologies", submitted to Progress in Photovoltaics. 2022.
58. IEC 61724-1:2021 Photovoltaic (PV) system performance—part 1: monitoring; international standard, Publication date: 2021-07-21, Edition 2.0, Solar photovoltaic energy systems, ICS 27.160 - Solar energy engineering, Stability date 2026.
59. Shoukry I, Libal J, Kopecek R, Wefringhaus E, Werner J. Modelling of bifacial gain for stand-alone and in-field installed bifacial PV modules. *Energy Procedia*. 2016;92:600-608. doi:10.1016/j.egypro.2016.07.025
60. Kreinin L, Bordin N, Karsenty A, Drori A, Grobgeld D, Eisenberg N. "PV module power gain due to bifacial design. Preliminary experimental and simulation data," 2010 35th IEEE Photovoltaic Specialists Conference. 2010:002171–002175. doi:10.1109/PVSC.2010.5615874
61. Frischknecht R, Itten R, Sinha P, et al. "Life cycle inventories and life cycle assessments of photovoltaic systems", Report IEA-PVPS T12-19:2020, December 2020.

How to cite this article: Tous L, Govaert J, Harrison S, et al. Overview of key results achieved in H2020 HighLite project helping to raise the EU PV industries' competitiveness. *Prog Photovolt Res Appl*. 2023;1-19. doi:10.1002/pip.3667